HHS Public Access

Author manuscript

ACS Infect Dis. Author manuscript; available in PMC 2024 January 11.

Published in final edited form as:

ACS Infect Dis. 2019 August 09; 5(8): 1456–1470. doi:10.1021/acsinfecdis.9b00156.

Design and Application of a High-Throughput, High-Content Screening System for Natural Product Inhibitors of the Human Parasite *Trichomonas vaginalis*

Jarrod B. King[†,‡], **Adam C. Carter**[†,‡], **Wentao Dai**[†,‡], **Jin Woo Lee**[†], **Yun-Seo Kil**[†], **Lin Du**[†], **Sara K. Helff**[†], **Shengxin Cai**[†], **Brandt C. Huddle**[†], **Robert H. Cichewicz**[*,†]

[†]Natural Products Discovery Group, Institute for Natural Products Applications and Research Technologies, Department of Chemistry and Biochemistry, Stephenson Life Sciences Research Center, 101 Stephenson Parkway, Room 1000, University of Oklahoma, Norman, Oklahoma, 73019, United States

Abstract

It is estimated that *Trichomonas vaginalis* affects an astonishing 3.9% of the world's population, and while many of those infected are asymptomatic, progression of the disease can lead to serious health problems. Currently, the nitroimidazoles constitute the only drug class approved to treat trichomoniasis in the United States, which makes the spread of drug resistance a realistic concern. We developed a new image-based, high-throughput, high-content assay for testing natural products (purified compounds and extracts) for antitrichomonal activity. Applying this assay system to a library of fungal natural product extracts led to the identification of three general classes of natural product inhibitors that exhibited moderate to strong activities against *T. vaginalis*: anthraquinones, xanthone-anthraquinone heterodimers, and decalin-linked tetramic-acid-containing metabolites. The tetramate natural products emerged as the most promising candidate molecules with pyrrolocin A (**51**) exhibiting potent activity against the parasite (EC_{50} = 60 nM), yet this metabolite showed limited toxicity to mammalian cell lines (selectivity index values of 100 and 167 versus 3T3 fibroblast and Ect1 normal cervical cells, respectively). The imaging-based assay system is a powerful tool for the bioassay-guided purification of single-component antitrichomonal biomolecules from complex natural product mixtures.

Keywords

Trichomonas vaginalis ; natural products; fungi; quinones; tetramic acid

[*]**Corresponding Author** rhcichewicz@ou.edu. Tel: 405-325-6969. Fax: 405-325-6111.

[‡]W.D., A.C., and J.K. contributed equally to this work.

The authors declare no competing financial interest.

ASSOCIATED CONTENT

Supporting Information

The Supporting Information is available free of charge on the ACS Publications website at DOI: 10.1021/acsinfecdis.9b00156. Bioactive compounds from the pure compound screening in *T. vaginalis*; Structures and therapeutic indices for quinones and related structures; Comparison of antitrichomonad activity of xanthoquinodin A1 (**46**) and **47** under anaerobic conditions; LC-ESIMS analysis of FDAA derivatives of beauversetin (**53**), equisetin (**48**), and 5'-epipyrrolocin A (**52**) derived hydrolysates; Effects of xanthoquinodin A1 (**46**) and beauversetin (**53**) on the growth of *T. vaginalis* under test conditions involving different oxygen levels; 1D, 2D NMR spectra and HRESIMS data for compounds **47**, **52**, and **54**

Trichomonas vaginalis is the most frequently encountered sexually-transmitted parasite in the United States.[1] Those infected by the parasite exhibit an increased risk for (i) HIV infection, (ii) development of cervical cancer, and (iii) infertility, as well as certain adverse pregnancy outcomes including (iv) miscarriage and (v) low-preterm birth weight.[2] Current clinical treatment options are limited to antiprotozoal nitroimidazoles (i.e., metronidazole and tinidazole), which still offer appreciably high levels of clinical efficacy (>90% of patients are cleared of the infection after a single course of treatment).[3–5] However, concerns have arisen that in addition to several noted side effects (e.g., nausea, vomiting, and others), the nitroimidazoles may possess carcinogenic and mutagenic properties.[6–7] This has led to worry about nitroimidazole treatment during pregnancy, as well as some apprehension about their use in the general population.[6] A rather troubling problem, which came to light based on surveillance data collected from patients infected with *T. vaginalis* and who received standard courses of nitroimidazole treatment, is the high rate of infection recurrence (5–31% in women).[5] While a portion of disease recurrence is attributable to further contact with untreated sexual partners, data suggests that a yet unknown proportion of *T. vaginalis* cases has the capacity to develop into persistent infectious states, which raises concerns about the clinical limitations of nitroimidazole therapies.[8] Even more concerning, nitroimidazole resistance has been detected in up to 9.6% of clinical *T. vaginalis* isolates, raising alarm that nitroimidazoles might become clinically less effective.[9–10] Considering the noted safety concerns and troubling clinical observations, there is a need for new disease management options that extend beyond the nitroimidazoles for treating *T. vaginalis* infections.

An examination of the research literature has revealed surprisingly sparse information concerning efforts to identify new classes of antiprotozoal molecules active against *T. vaginalis*, with only a small fraction of those endeavors dealing with natural products.[11–12] A handful of prior studies had focused exclusively on testing plant extracts,[13–16] but revealed little about the molecules responsible for their inhibitory effects. In a few instances, chemically-driven investigations of extracts have yielded a handful of secondary metabolites possessing activity against *T. vaginalis* including berberine,[17] (−)-usnic acid,[18] emodin,[19] hamycin,[20] hederagin,[21] and mulinolic acid;[22] however, these compounds suffer from poor potency and lack selectivity compared to metronidazole. Although the limited scope of reports pertaining to the discovery of new leads to fight *T. vaginalis* infections is worrisome, it also signals the potential that exists to identify new bioactive compounds for development into clinically useful agents. This expectation is reasonable, especially for natural products, which have long served as an outstanding resource for the discovery of new antiinfectious agents including some of the topmost antiparasitic compounds in current clinical use (e.g., avermectins, artemisinin, and more).[23–24]

Aside from the scarcity of natural-product-focused drug discovery efforts concentrating on inhibiting of *T. vaginalis*, there are relatively few reports of vetted assay methods that are amenable to the systematic screening and identification of compounds that inhibit this unique parasite. Most of the reported methods had employed manual microscopy-based approaches for cell enumeration[25–26] or used metabolically-activated dyes such as resazurin as indicators of parasite viability.[25–26] With this in mind, we set about developing an assay system that (i) was able to reliably identify samples containing antitrichomonal

compound(s), (ii) was amenable to high-throughput sample testing, (iii) could accurately distinguish between complete versus partial inhibition of *T. vaginalis*, and (iv) was applicable for use involving a wide variety of sample types including pure compounds and natural product extracts. Herein we report the results of our assay development program, as well as describe new natural product scaffolds that exhibit promising inhibitory activities against *T. vaginalis*.

RESULTS AND DISCUSSION

Development of an Assay for Detecting *T. vaginalis* Inhibitors.

Resazurin-based colorimetric assays are widely used in bioactive compound screening campaigns to identify substances that inhibit cell viability and proliferation under aerobic and anaerobic conditions.[27] This dye and its H_2O soluble salts are readily reduced by NADH to yield the red, fluorescent product resorufin. Despite its reported use for the identification of *T. vaginalis* inhibitors, we were surprised to discover that, in our hands, this reagent was rather insensitive for the detection of reasonably large numbers of viable cells. We observed that under anaerobic assay conditions, a population of ~10,000 trichomonads per well in a 96-well microtiter plate was needed as a threshold to consistently signal a positive response for the presence of live *T. vaginalis*. Given that we established an inoculum of 40,000 trichomonads per well as an optimal starting point for assays, it meant that compounds affording modest (~75%) parasite-kill rates would be indistinguishable from more potent and potentially better agents (Figure 1). Therefore, we set about designing a new assay system that was more sensitive, as well as able to handle a wide-range of complex test substances (e.g., pure compounds and extracts containing colored or UV-active natural products).

One method deemed to be a promising alternative to the resazurin assay was high-content imaging.[28] We speculated that this approach would offer a more responsive tool for evaluating the live/dead-status of individual trichomonads within sample populations. However, we quickly recognized that live trichomonads were not fully compatible with imaging-based detection methods; the rapid movements of the flagellated parasites caused the cells to severely blur even with a reasonably fast exposure time (10 ms). Accordingly, we identified a method to fix the trichomonads with glutaraldehyde followed by the application of a dual cell-staining system consisting of acridine orange (cell-permeable DNA stain) and propidium iodide (DNA stain that is not permeant to live cells) for live/dead determination (Figure 2). Initial tests conducted using the Operetta (PerkinElmer) high-content imaging system revealed that this assay tool could detect as few as one live or dead trichomonad per image field and was robust (Z-factor of 0.92). Moreover, this type of detection system was amenable to high-throughput screening of *T. vaginalis* viability, especially with UV/VIS-active natural products since the stored image files (i.e., two image fields recorded per well) could be manually inspected to identify potential false-positive and false-negative results. Additionally, DMSO was determined to be an acceptable vehicle for compound testing since a concentration of 1% by volume appeared to have no detrimental impact on the viability of *T. vaginalis* cells.

Testing Purified Natural Products.

To examine the probative capabilities of the new *T. vaginalis* imaging-based assay, a focused library of chemically diverse natural products was tested. The compound library consisted of 430 metabolites sourced by our research team from marine organisms, plants, bacteria, and fungi. An initial high-dose concentration (100 μM) was chosen to afford the opportunity to evaluate several challenging screening scenarios, especially those involving potential false-positives brought about by compound precipitation and UV/VIS-interference. The imaging-based assay proved invaluable since all the data files corresponding to potential hits (i.e., compounds that provided inhibition exceeding that afforded by 25 μM metronidazole) were immediately available for inspection to confirm that the number of live trichomonads had been reduced. This test revealed that 64 of the compounds we tested exhibited activities that were equal to or better than the positive control. The large number of active samples was not unexpected since our pure compound library was largely populated by bioactive substances that had previously demonstrated cytotoxicity toward mammalian cells and/or inhibited the proliferation of various microorganisms. To refine the list of natural products further, the hit compounds were screened at 25 μM, which resulted in a subset of 9 compounds that exhibited activities comparable to 25 μM metronidazole (Figure S1, Supporting Information). These results also reinforced the need for a mammalian cell-based cytotoxicity counter screen to aid in the elimination of undesirable non-specific cellular toxins. Accordingly, the 9 hits were tested over a wide-range of concentrations extending two-orders of magnitude (0.25–25 μM) against both *T. vaginalis* and a normal mouse fibroblast (NIH/3T3) cell line. With these data in hand, the EC_{50} values for all compounds against both the parasite and mammalian cells were estimated. The EC_{50} values were used to calculate a selectivity index (SI) value [SI_{3T3} = (EC_{50} for 3T3 cells)/(EC_{50} for *T. vaginalis*)] for each of the bioactive substances (Figure 3). While the SI values revealed that most of the pure natural products were equipotent inhibitors of trichomonads and mammalian cells, one noted exception was 2-bromoascididemin, which exhibited modest selectivity (SI_{3T3} = 14). Thus, we established that the new assay was amenable to the testing of structurally diverse natural products across a wide range of concentrations. Furthermore, when coupled with a mammalian cell cytotoxicity screen, it could reveal a substance's ability to selectively inhibit the target parasite.

Testing Fungal Natural Product Extracts.

The University of Oklahoma, Natural Products Discovery Group has generated a library of over 50,000 fungal extracts. Each extract consists of the organic residue obtained after a fungal isolate was cultured in small scale for 3 weeks on Cheerios breakfast cereal, extracted with EtOAc, and partitioned against H_2O. For testing purposes, a subset of 1,748 samples was selected for examination in the high-content-imaging assay system. For the first stage of testing, we determined that it was most efficient to screen extracts in duplicate at a single concentration (15 μg/mL). This provided 111 'hits' that inhibited the viability of *T. vaginalis* at levels equal to or better than the inhibition achieved using 25 μM metronidazole. These 'hit' extracts were subjected to a second stage of testing over a range of concentrations (0.15–15 μg/mL), which yielded 71 samples that retained potent activity and generated sigmoidal concentration-response curves. During this period in the assay development process, we considered the value of introducing a second mammalian cell type

for selectivity evaluation since fibroblasts cells, although capable of vigorous *in vitro* growth that made them simple to test, might not offer a level of cytotoxin sensitivity or exhibit cellular properties typically associated with cells at the sites of *T. vaginalis* infections. Thus, Ect1/E6E7 normal-type cervical cells were chosen to provide a second point of reference for selectivity testing. Accordingly, the EC_{50} value for each extract's parasite-inhibitory activity, as well as its cytotoxic effects toward Ect1/E6E7 cells were determined and the data were plotted as illustrated in Figure 4. This data visualization method provided a simple graphical means to identify samples that offered high levels of parasite inhibition yet exhibited limited toxicity toward mammalian cells. Thus, we proceeded to prioritize samples appearing in the upper right quadrant of the graph since those samples offered the best starting points for new bioactive compound discovery. Based on those data, three fungi responsible for generating potent and selective extracts were selected for follow-up chemical investigation including: two *Fusarium* spp. isolates (plate 55 well F11; SI_{Ect1} = 36 and plate 72 well E6; SI_{3T3} ≥2.7) and a *Humicola* sp. isolate (plate 78 well A3; SI_{3T3} = 25).

Bioassay-Guided Purification and Testing of Natural Products from *Fusarium sp.* Isolate A.

An extract prepared from *Fusarium* sp. isolate A was subjected to bioassay-guided fractionation using silica gel vacuum liquid chromatography (VLC), HP20SS VLC, and C_{18} HPLC chromatography yielding three quinone-containing natural products: fusarubin (**1**),[29] javanicin (**2**),[30] and solaniol (**3**)[31] (compounds were identified based on comparisons of experimental LC-ESIMS and NMR data to the published values)[32–33] (Figure 5). The purified metabolites exhibited a range of potencies against *T. vaginalis* with **1** and **2** being the most potent (EC_{50} values of 2.5 μM and 1.3 μM, respectively), while **3** showed greatly reduced activity (EC_{50} = 40 μM). Metabolite **1** stood apart from the other natural products with a SI_{Ect1} = 30, which greatly exceeded the SI values determined for **2** (SI_{Ect1} = 3.1) and **3** (SI_{Ect1} = 0.4) (Figure 5). These data initially suggested that simple quinone-containing scaffolds like **1** might serve as a starting point for the identification of structural analogues that offered improved selectivity and potency.

Exploring the Bioactivities for Analogues of Compound 1.

Based on the activities of natural products **1–3**, we proceeded to test 42 additional natural and synthetic compounds (compounds **4–45**, Table S1, Supporting Information) that shared many key structural elements with the metabolites obtained from *Fusarium* sp. isolate A to determine if compounds could be identified that afforded improved potency and selectivity. Although many of the tested molecules exhibited low-to-mid-micromolar inhibition of *T. vaginalis* viability, none of those compounds proved to be as selective as metabolite **1** (other compounds exhibited SI_{Ect1} values ≤4.5) (Figure 6). Results of the bioactivity assessment are summarized in Table S1 (Supporting Information). Notably, atovaquone (**37**),[34] a commercially available antiparasitic drug (used to treat some infections caused by *Babesia* spp., *Plasmodium* spp., and *Toxoplasma* spp.),[35] exhibited only modest activity and a poor SI_{Ect1} value of <0.1, suggesting that this compound did not offer a reasonable-level of crossover inhibition against *T. vaginalis*. Given that none of the tested compounds afforded more favorable activity compared to **1** (i.e., no improvement in potency or SI values), as well as redox-related concerns (e.g., potential for quinones

to react with nucleophilic amino acid residues, as well as a notorious history of problems in a variety of assays),[36] we became concerned that this scaffold might not provide a suitable opportunity for further development. To examine if redox activity might partially explain the activity of **1** and related compounds, we devised a test in which the potencies of compound **1**, 2-methoxynaphthazarin (**9**), and metronidazole were assessed under three atmospheric conditions with different oxygen levels (i.e., aerobic, microaerophillic, and anaerobic). The results of those tests revealed that the activities of **1** and **9** both decreased as oxygen was introduced into the test culture conditions (Figure 7). Curiously, compounds **1** and **9** differed in another respect; **1** was only able to afford the partial elimination of trichomonads under strict anaerobic condition, whereas **9** was able to provide for the complete elimination of the parasite in an anaerobic atmosphere. In contrast, metronidazole maintained consistent potency across all the tested atmospheric conditions (Figure 7). Given the expected heterogeneity of oxygen levels across the various body sites infected by *T. vaginalis*, we abandoned further pursuit of **1** and its analogues in favor of other, more promising compounds.

Bioassay-Guided Purification and Testing of Natural Products from a *Humicola* sp. Isolate.

The extract prepared from the *Humicola* sp. isolate was subjected to bioassay-guided fractionation using silica gel vacuum liquid chromatography (VLC), HP20SS VLC, and C_{18} HPLC purification steps to afford the xanthone-anthraquinone heterodimer xanthoquinodin A1 (**46**), which was identified by comparisons of its experimental ^{1}H and ^{13}C NMR spectra, LC-ESIMS data, and specific rotation value to the published values.[37] Compound **46** was tested for activity against *T. vaginalis,* as well as counter-screened against Ect1/E6E7 cells, which revealed the natural product had a favorable SI_{Ect1} of ~20. Based on our prior experiences with redox-active compounds (*vide supra*), **46** was tested under aerobic, microaerophillic, and anaerobic conditions to determine how those changes would influence its activity. To our surprise, compound **46** maintained consistent potency under all experimental conditions (average EC_{50} = 3 μM) (Figure S28, Supporting Information), which suggested that this compound functioned in a manner that was different than **1** and its analogues.

Reduction of Xanthoquinodin A1.

While the activity of **46** was different compared to the simple quinones that we had tested, we were interested in determining how this compound would work if it were subjected to chemical reduction. For that reason, compound **46** was treated with sodium borohydride to provide **47** (Scheme 1). Analysis of the ^{13}C NMR data for **47** revealed the loss of a carbonyl chemical shift relative to **46** with the concomitant addition of a new spin at δ_C 71.9. Follow-up HSQC and HMBC experiments [e.g., correlation from H-10' (δ_H 5.04) → C-13 (δ_C 30.5)] and ROESY [e.g., cross-peak observed between H-10' ↔ H-4' (δ_H 6.47)] confirmed that the C-10' carbonyl in **46** had been stereospecifically reduced to an alcohol yielding a single isomeric product. Testing revealed that the inhibitory activity of **47** against *T. vaginalis* (EC_{50} = 3 μM) was indistinguishable from **46** (Figure S8, Supporting Information). This indicated that unlike compounds **1–45**, the activity of natural product **46** may not be as susceptible to redox-dependent processes.

Establishing an Antibacterial Counter-Screen with *Lactobacillus acidophilus*.

While the antitrichomonal activity of **46** appeared promising, it was not apparent what effect this and other compounds we anticipated discovering would have on a person's microflora. This was a concern because microbiome disruption can have deleterious consequences for patients following antibiotic treatment.[38] For that reason, *Lactobacillus acidophilus* was chosen as a representative bacterium species because of its widespread occurrence in the human mouth, intestinal tract, and vagina.[39] Unfortunately, compound **46** was determined to exhibit near equipotent activity against *T. vaginalis* and *L. acidophilus* (Figure 8). In contrast, metronidazole showed no inhibition of the bacterial indicator strain at the concentrations tested, although this compound does inhibit other bacteria.[40] Consequently, **46** was dropped from further consideration given the negative impact that its antibacterial activity might have on the stability of a patient's microflora.

Bioassay-Guided Purification and Testing of Natural Products from *Fusarium* sp. Isolate B.

A crude extract prepared from *Fusarium* sp. isolate B was subjected to bioassay-guided fractionation using silica gel vacuum liquid chromatography (VLC), HP20SS VLC, and C_{18} HPLC to afford the compound equisetin (**48**). In the process of obtaining **48**, 5'-epiequisetin (**49**) was also purified from the extract since its LC-ESIMS data had provided evidence that it was likely a structural analogue of the bioactive constituent. The purified compounds were identified by comparisons of their ^{1}H and ^{13}C NMR spectra and HRESIMS data to published values.[41] The absolute configurations of the tetramic acid portions of both compounds were determined using a previously described oxidative bond-cleavage and LC-ESIMS-facilitated analysis methodology.[42–43] Testing of the purified compounds revealed a stark difference in their respective antitrichomonal activities; whereas **48** exhibited rather potent inhibitory effects (EC_{50} = 3 μM) with good selectivity (SI_{3T3} = 33), **49** was inactive at concentrations up to 25 μM. An examination of both metabolites revealed that the remarkable difference in their biological activities could be traced to the epimerization of a single stereocenter (5'*S* in **48** and 5'*R* in **49**). Taking these data into consideration, as well as noting that **48** was non-toxic to *L. acidophilus* at concentrations up to 50 μM (Table 3), there was ample reason to believe that further exploration of this family of natural products had the potential to provide additional bioactive analogues.

To facilitate the identification of other natural products containing a tetramate linked to a *trans*-decalin system, we turned to our extensive library of fungal isolates and their associated chemical data. This family of natural products has been reported from a taxonomically diverse assemblage of fungi[41–42, 44–46] and our records revealed that we had previously encountered these compounds from several fungal isolates in our collection. After considering the range of structural variation that we could anticipate from the fungal isolates available to us, 4 fungi were selected to serve as the subjects of a targeted (chemically-guided) purification process: (i) *Fusarium* sp. isolate C, (ii) *Penicillium* sp., (iii) *Alternaria* sp., and (iv) *Phoma* sp. P34E5. Those efforts led to the purification of 7 additional tetramic-acid-containing metabolites including trichosetin (**50**),[45] pyrrolocin A (**51**),[42] 5'-epipyrrolocin A (**52**) (new), beauversetin (**53**),[46] 5'-epibeauversetin (**54**) (new), phomasetin (**55**),[44] and 5'-epiphomasetin (**56**)[44] (Figure 9 and Table 3). Whereas the previously reported tetramic acid metabolites were identified based on comparisons of their experimental versus

published spectrometry and spectroscopy data, the new analogues became the foci of our structure determination efforts.

Compound **52** (purified from the *Penicillium* sp. isolate) was obtained as a pale yellow solid. Its molecular formula was deduced from HRESIMS data to be $C_{27}H_{39}NO_5$ ($[M-H]^-$ ion at *m/z* 456.2747, calcd for 456.2755). The ^1H and ^{13}C NMR data (Tables 1 and 2) revealed the presence of eight olefinic carbons, an oxygenated methylene, an oxygenated methine, and 5 methyl groups. Comparison of the 1D NMR data of **52** with compound **51** (isolated from the same fungus) indicated that the only noteworthy difference in the ^{13}C NMR data for these two molecules was that the carbon spin resonating at δ_C 68.1 in compound **51** now appeared at δ_C 67.4 in metabolite **52**. Combining this information with the bond-line structure established for **52** (based on analyses of its ^1H-^1H COSY, HSQC, and HMBC data, Figure 10A), it was proposed that the new natural product was the 5'-epimer of **51**.

Upon probing the stereochemical properties of compound **52**, the relative configuration of the decalin system was affirmed based on ^1H-^1H ROESY correlations detected between the following sets of protons: Me-12 ↔ H-6 and H-3; H-10ax ↔ H-6, H-7eq, and H-8; as well as H-7ax ↔ H-10eq and H-11 (Figure 10A). The absolute configuration of this moiety was determined by comparing its CD spectrum with data obtained for similar metabolites. Specifically, the positive Cotton effects at 234 and 291 nm indicated that the absolute configuration of the decalin-ring portion of this structure was 2*R*,3*S*,6*R*,8*S*,11*S* (Figure 12, Figures S31 and S32, Supporting Information).[42] The absolute configuration of the hydroxy group on the olefinic side chain was determined to be 18*R* based on an analysis employing the modified Mosher reaction (Figure 11).[42, 47] The absolute configuration of C-5' was determined by oxidative bond cleavage of the tetramic acid ring followed by acid hydrolysis to yield *N*-Me-serine.[42–43] Marfey derivatization of the *N*-Me-serine was performed and the product was analyzed by LC-ESIMS together with the derivatized products generated from both *N*-Me-L- and D-serine standards. The *N*-Me-D-serine was made by racemization of commercially available *N*-Me-L-serine using acetic acid and salicylaldehyde as described previously.[48–49] The resulting amino acid residue was determined to be *N*-Me-L-serine, thus, the absolute configuration of **52** was assigned as 2*R*,3*S*,6*R*,8*S*,11*S*,18*R*,5'*S*.

Compound **54** was purified as a pale yellow solid. Its molecular formula was deduced as $C_{24}H_{33}NO_4$ based on HRESIMS data. The ^1H NMR spectrum of **54** (Table 1) showed thirty-one proton signals including 5 aromatic protons and 4 methyl spins. The ^{13}C NMR spectrum (Table 2) contained 24 carbon spins, which were later classified according to their multiplicities using an HSQC experiment. Those data indicated that **54** was structurally similar to **52**. Based on 2D NMR (^1H-^1H COSY, HSQC, and HMBC) data (Figure 10B), the bond-line structure of **54** was confirmed to be the same as metabolite **53**, which indicated that this compound was likely to be another 5'-epimer.

The relative configuration of the decalin moiety was deduced as 2*R**,3*S**,6*R**,8*S**,11*S** based on the key ^1H-^1H ROESY correlations between Me-12 ↔ H-3 and H-6, H-6 ↔ H-9eq, H-6 ↔ H-8, as well as H-11 ↔ H-7ax and H-9ax (Figure 10B). The positive Cotton effects recorded for **54** at 234 and 289 nm indicated that the absolute configuration of the decalin moiety in **54** was the same as that in compound **53** (Figure 13). Further analysis

of key ROESY correlations including H-15 ↔ H-13 and Me-17 revealed both exocyclic olefins (Δ^{13} and Δ^{15}) had *trans* geometries. Using the same oxidative bond cleavage and LC-ESIMS analysis method that had been applied to the tetramic acid moiety in metabolite **52**, the absolute configurations of C-5' stereocenters were determined as 5'*R* (**53**) and 5'*S* (**54**), respectively.[42–43, 49] Thus, the absolute configuration of **54** was determined to be 2*R*,3*S*,6*R*,8*S*,11*S*,5'*S*.

Assessing the Biological Activities of the Tetramic-Acid-Containing Natural Products.

The antitrichomonal effects of the tetramic-acid-containing natural products were evaluated revealing an intriguing trend; whereas several of the compounds exhibited potent activities with EC_{50} values at or below single digit micromolar concentrations (i.e., **48**, **50**, **51**, **53**, and **55**) their 5'-epimers were inactive even at concentrations as high as 25 μM (Table 3). The three most potent molecules, **51** (EC_{50} = 0.060 μM), **53** (EC_{50} = 0.80 μM), and **55** (EC_{50} = 0.35 μM), revealed that the tetramic-acid-containing molecules were among the most potent *T. vaginalis* inhibitors we have observed to date. To determine if the *Trichomonas*-inhibitory effects of the tetramic acid natural products were affected by the presence of molecular oxygen, metabolite **53** was tested under aerobic, microaerophilic, and anaerobic conditions (Figure S29, Supporting Information). Unlike many of the other compounds that we tested, **53** maintained potency under all the test atmospheric conditions exhibiting no statistically significant change in EC_{50} value, as well as affording the complete elimination of the parasite. Although some tetramic-acid-containing compounds have been reported to possess antibacterial activities,[50–51] none of the compounds that inhibited *T. vaginalis* inhibited *L. acidophilus* at 50 μM (Figure 8). The selectivity of the tetramic-acid metabolites for *T. vaginalis* versus mammalian cells also appeared favorable (Table 3) with relatively large SI values for compound **51** (SI_{3T3} = 100, SI_{Ect1} = 167). Based on these data, the tetramic-acid-containing natural products exhibited many promising characteristics that highlight their potential for further development as inhibitors of *T. vaginalis*.

CONCLUSIONS

A rapid and sensitive assay for the detection of *T. vaginalis* inhibitors was developed and used to test a variety of substances varying from pure compounds to complex fungal extracts. In the process of screening a portion of our fungal extract library, we detected and went on to purify several natural products that exhibited inhibitory activities against *T. vaginalis* and were relatively non-cytotoxic to human Ect1/E6E7 cells. In parallel to their PAINS-like qualities, quinone-containing compounds[36, 52] were generally found to be problematical starting points for the development of new antitrichomonal scaffolds since their inhibitory properties were significantly influenced by the relative amounts of oxygen the trichomonads were exposed to throughout the assay period. Moreover, these types of rather promiscuous compounds exhibited antibacterial activities against *L. acidophilus* suggesting that their non-specific antibiosis effects could upset the microbiome structures of patients, thus creating new potential problems.

Based on the lessons learned from the quinones, we proceeded to test a second group of more promising tetramic-acid-containing natural products as inhibitors of *T. vaginalis*. A

striking feature of their antitrichomonal effects was the decided difference in the biological activities of the 5'-epi-isomers, which generally showed no inhibitory effects against *T. vaginalis*. Compound **51** emerged as a rather promising metabolite based on its potent activity against the parasite (EC_{50} = 0.060 μM) and limited toxicity against both the human Ect1/E6E7 cervical cell line (SI = 167) and *L. acidophilus* (EC_{50} > 50 μM). Although our testing was limited to 9 tetramic-acid-containing natural products, the data suggested that modifications to the C-3 group of the *trans*-decalin system may provide additional opportunities for generating new analogues that offer even further improvements in potency and selectivity.

EXPERIMENTAL SECTION

General Experimental Procedures.

UV data were recorded on a Hewlett Packard 8452A diode array spectrophotometer. Optical rotation measurements were made on an AUTOPOL® III automatic polarimeter. The LC-ESIMS analyses were performed on a Shimadzu UFLC system with a quadrupole mass spectrometer using a Phenomenex Kinetex C_{18} column (3.0 mm × 75 mm, 2.6 μm) and MeCN-H_2O (0.1% HCOOH) gradient solvent system. HRESIMS spectra were measured using an Agilent 6538 Ultra High Definition (UHD) Accurate-Mass Q-TOF system. NMR spectra were obtained on Varian spectrometers (500 MHz and 400 MHz for ^1H, and 100 MHz for ^{13}C) using DMSO-d_6 and $CDCl_3$ as solvents. Column chromatography was conducted using silica gel and HP20SS. HPLC was performed on a Waters System equipped with a 1525 binary HPLC pump coupled to a 2998 PDA detector with a Phenomenex Gemini C_{18} column (21.2 × 250 mm or 10 × 250 mm, 5 μm particle size).

Culture of Organisms.

Trichomonas vaginalis Donne (PRA-98) was purchased from the American Type Culture Collection (ATCC, Bethesda, MD). After some investigation, Keister's Modified TYI-S33 medium[53] (adjusted to pH 6.0 and without Diamond's vitamin solution) was determined to be the optimum medium to support the growth of *T. vaginalis*. The medium was filter sterilized and aliquots stored frozen for later use. A notable difference in the growth of *T. vaginalis* was observed dependent upon the source from which the bovine bile obtained. The best growth of *T. vaginalis* was observed when Sigma B8381 bovine bile was used and it was adopted as the sole bovine bile source for all experiments. For culture maintenance and propagation, trichomonads were grown in a 37 °C incubator in sealed screw cap tubes. For microtiter plate assays, trichomonads were tested under several atmospheric conditions including standard atmospheric condition (aerobic atmosphere: ~21% O_2, 0.04% CO_2), candle jar (microaerophilic atmosphere: ~10% O_2, 5% CO_2), BD GasPak EZ Campy sachets (microaerophilic atmosphere: 6–16% O_2, 2–10% CO_2), and BD GasPak EZ Anaerobe sachets (anaerobic atmosphere: O_2 at nondetectable level, >13% CO_2). Unless specified, assays were carried out in conditions employing reduced levels of oxygen and increased levels of carbon dioxide (microaerophilic), which stimulates *Trichomonas* growth.[54]

NIH/3T3 (CRL-1658) mouse fibroblast and Ect1/E6E7 (CRL-2614) normal-type human ectocervical cell lines were purchased from ATCC. NIH/3T3 cells were maintained in

Dulbecco's Modified Eagle's medium with 5% FetalClone III (Hyclone) and Ect1/E6E7 cells in keratinocyte-serum free medium (K-SFM, GIBCO-BRL 17005-042) or RPMI 1640 medium with 5% FetalClone III and supplemented with EGF (10 ng/mL Novoprotein C029).

Lactobacillus acidophilus (ATCC 4356) was purchased from ATCC. The bacterium was maintained and tested on MRS agar and broth at 37 °C under anaerobic conditions (BD GasPak EZ Anaerobe sachets).

Trichomonas vaginalis Assays.

For assays, a 250 μL aliquot of *T. vaginalis* cryopreserved in liquid N_2 with 5% dimethyl sulfoxide (DMSO) of was thawed rapidly at 37 °C and put into a screw cap tube containing 12 mL of pre-warmed modified TYI-S-33 medium. The sample was incubated for 24 h at which point confluent growth of the parasite had occurred and live trichomonads were counted. A typical count yielded > 3.0×10^7 cells per tube. Stock cultures were diluted in fresh medium to achieve 40,000 trichomonads per 100 μL of medium in each well of a 96-well microtiter plate. Pin tools and pipets were used to dispense extracts and pure compounds dissolved in DMSO. Throughout the assay setup process, trichomonads were exposed to normal atmospheric conditions for not more than 30 min before experiments commenced. The trichomonads were determined to tolerate 1% DMSO with no detectable negative effects (no changes to the number of live trichomonads). Accordingly, all experiments were conducted so that the amount of DMSO did not exceed 1% by volume. All plates contained vehicle-only (DMSO) and positive (25 μM metronidazole) controls to ensure that the biological response of the trichomonads were consistent across assays using identical test conditions. For candle jar assays, plates were placed in a humidified candle jar, the candle was lit, and the jar was sealed before being placed in a 37 °C incubator for a 17 h incubation period. For assays using BD GasPak, the manufacturer's instructions were followed as provided. After 17 h of incubation, microtiter plates were removed and 100 μL of room temperature fixation solution added to each well. The fixing solution was a PBS based solution developed in our lab that contained 1% glutaraldehyde, 5 μM propidium iodide, and 5 μM acridine orange (HCl salt). This solution was found to be stable at room temperature for several months and it lasted even longer when stored in a refrigerator. Plates treated with fixing solution were placed on an orbital shaker for 30 s to disperse clumps of cells and then moved to an incubator for 3 h for staining and fixation to occur. The plates were quantitatively imaged using the Perkin Elmer Operetta and analyzed using the Harmony 3.5.1 software package. Quantification involved the software identifying all trichomonads and subtracting live (green only) from dead (green and red) cells using a propidium iodide threshold of less than 6500 units; this threshold was determined to enable the assessment of membrane integrity and thus served as an indicator of live versus dead cells.

A traditional resazurin based assay employing a plate reader for live cell quantification was also performed.[26] Trichomonads were grown in microtiter plates and at the end of experiments, 10 μL of a 0.1 mg/mL resazurin stock in PBS was added to each well. Plates were incubated at room temperature in the dark for 1 h. At the end of the incubation period,

the plates were shaken and analyzed on a fluorescence plate reader (Tecan Infinite M200) with a 556 nm excitation wavelength and an emission of 590 nm.

Mammalian Cell Cytotoxicity Assays.

Mammalian cell assays were performed as described previously[55] and viability determined by MTT assay[56] or by a Calcein AM and Hoechst 33342 live cell area assay using an Operetta system. Assays were performed by adding to each well of the microtiter plate 5 μL of a 40 μM Calcein AM and 160 μM Hoechst 33342 stock solution prepared in DMSO that was diluted (1:5) in PBS buffer. After treatment, plates were incubated for 30 min before being analyzed on the Operetta system. Harmony software was used to calculate the live cell area by finding all Hoechst-labeled nuclei and the cells were assigned live or dead status based on their degree of green fluorescence. Live cells contain esterases that cleave the AM group from Calcein AM causing the cells to glow bright green.

Lactobacillus acidophilus Viability Assay.

Colonies of *L. acidophilus* were sampled with a loop and used to inoculate 10 mL of MRS broth and then vortexed. 100 μL aliquots were added to each well of a 96-well microtiter plate. Test compounds were dissolved in DMSO (0.5% final concentration DMSO) and added to the wells. Plates were read on a microplate reader at 600 nm to establish baseline absorbance (dispersion) values for each well, the plates were incubated at 37 °C for 18 h, and their contents analyzed on the microtiter plate reader at 600 nm to determine changes in their optical density values.

Purification of Secondary Metabolites 1–3.

A fungal isolate, *Fusarium solani* (internal strain designation Tree 400 EW+PNGP-3), identified based on its ribosomal internal transcribed spacer (ITS) sequence data (GenBank accession number MK424121), was obtained from a soil sample collected under a tree in the Oliver Wildlife Preserve in Norman, Oklahoma. This isolate was grown for 4 weeks on Cheerios breakfast cereal supplemented with a 0.3% sucrose solution with 0.005% chloramphenicol in three large mycobags (Unicorn Bags, Plano, TX) prior to being homogenized, extracted, and partitioned with EtOAc. The EtOAc soluble material (40.4 g) was subjected to silica gel vacuum liquid chromatography with elution steps of 1:1 hexanes/DCM, DCM, 10:1 DCM/MeOH, and MeOH, yielding 4 fractions. The 10:1 DCM/MeOH fraction (7.8 g) was subjected to HP20SS vacuum liquid chromatography and eluted with a step gradient of MeOH in H_2O (30%, 50%, 70%, 90%, and 100%) and 1:1 DCM/MeOH, yielding a total of 6 fractions. Bioassay analysis of the resulting fractions indicated *T. vaginalis*-inhibitory activity was concentrated in the 90% MeOH fraction. This fraction was subjected to further bioassay-guided purification using preparative C_{18} HPLC (250 mm × 21.2 mm, 5 μm) with a MeOH-H_2O gradient (30:70 to 100:0), followed by isocratic semi-preparative C_{18} HPLC (250 mm × 10 mm, 5 μm) with MeCN-H_2O containing 0.1% HCOOH (50:50) to yield three known bioactive naphthoquinones [**1** (1.5 mg), **2** (1.8 mg), and **3** (3.0 mg)].

Testing of Additional Commercially Available and Synthesized Quinones.

The structures of compounds **4–45** are shown in Table S1, Supporting Information. The identities of synthesized compounds were confirmed through ^{1}H NMR, as well as by comparisons to additional spectroscopic data as reported in the literature.

Synthesis of Naphthopurpurin (8).

Compound **8** was synthesized according to a previously reported procedure.[57] Specifically, 153 mg of naphthazarin (0.80 mmol) was dissolved in 45 mL of aqueous KOH (2 M). The solution was stirred vigorously and refluxed for 4 h. After cooling to ambient temperature, glacial acetic acid was used to neutralize the reaction mixture, resulting in a color change from purple to red. The reaction mixture was partitioned with 4 × 40 mL of chloroform. The aqueous phase was acidified with 5 mL of HCl (1 M) and partitioned with 4 × 50 mL of EtOAc. The organic phases were combined and the solvent was removed under vacuum to yield naphthopurpurin (130 mg, 78% yield). ^{1}H NMR (400 MHz, $CDCl_3$): 12.74 (s, 1H), 11.47 (s, 1H), 7.34 (d, J = 9.5 Hz, 1H), 7.21 (d, J = 9.5 Hz, 1H), 6.37 (s, 1H).

Synthesis of 2-Methoxynaphthazarin (9).

Compound **9** was synthesized according to a previously reported procedure.[58] Specifically, 120 mg of naphthopurpurin (0.58 mmol) was dissolved in 5 mL of absolute MeOH and 80 μL of HCl (12 M). The solution was stirred and refluxed for 4 h, then brought back to room temperature. The product was purified from the reaction mixture by silica gel vacuum liquid chromatography using a stepwise gradient (hexanes, 3:1 hexanes/EtOAc, 2:1 hexanes/EtOAc, 1:1 DCM/MeOH, and MeOH). From the 3:1 hexanes/EtOAc fraction, 2-methoxynaphthazarin was obtained (17 mg, 13% yield). ^{1}H NMR (400 MHz, $CDCl_3$): 12.63 (s, 1H), 12.16 (s, 1H), 7.27 (d, J = 9.5 Hz, 1H), 7.20 (d, J = 9.5 Hz, 1H), 6.16 (s, 1H), 3.93 (s, 3H).

Synthesis of 1,4-Dihydro-5,8-dihydroxy-2-methyl-9,10-anthracenedione (10).

Compound **10** was synthesized according to a previously reported procedure.[59] Specifically, 157 mg of naphthazarin (0.83 mmol) was dissolved in 5 mL glacial acetic acid. To this solution, 200 μL of isoprene (2.0 mmol) was added, and the mixture was stirred with heating to 70 °C for 48 h. The product was semi-purified from the reaction mixture by silica gel vacuum liquid chromatography, eluted with 25:1 hexanes/EtOAc, yielding a crude mixture of products. The mixture was dissolved in 5 mL of aqueous KOH (2 M) and stirred vigorously for 30 min. HCl (1 M) was added to acidify the solution, which was gravity filtered to yield 1,4-dihydro-5,8-dihydroxy-2-methyl-9,10-anthracenedione (38 mg, 18% yield). ^{1}H NMR (400 MHz, $CDCl_3$): 12.54 (s, 2H), 7.21 (s, 2H), 5.55 (m, 1H), 3.25 (m, 2H), 3.14 (m, 2H), 1.82 (s, 3H).

Synthesis of 1,4-Dihydro-2-methyl-9,10-anthracenedione (11).

Compound **11** was synthesized according to a previously reported procedure.[59] Specifically, 187 mg of 1,4-naphthoquinone (1.2 mmol) was dissolved in 5 mL glacial acetic acid. To this solution, 200 μL of isoprene (2.0 mmol) was added, and the mixture was stirred with heating to 70 °C for 48 h. To the reaction mixture, 5 mL of H_2O were added and the mixture was

cooled to 0 °C. The mixture was gravity filtered to yield a crude mixture of products. The mixture was dissolved in 5 mL of aqueous KOH (2 M) and stirred vigorously for 15 min. The solution was acidified with 1 mL of HCl (12 M). The resulting solution was gravity filtered to yield 1,4-dihydro-2-methyl-9,10-anthracenedione (95 mg, 35% yield). ^{1}H NMR (400 MHz, $CDCl_3$): 8.07 (m, 2H), 7.69 (m, 2H), 5.54 (m, 1H), 3.23 (m, 2H), 3.12 (m, 2H), 1.80 (s, 3H).

Purification of Secondary Metabolite 46.

A fungal isolate, *Humicola grisea* (internal strain designation Mystery-9 SEA-2), was identified based on its ribosomal internal transcribed spacer (ITS) sequence data (GenBank accession number MK424122). The fungus was grown for 4 weeks on Cheerios breakfast cereal supplemented with a 0.3% sucrose solution containing 0.005% chloramphenicol in three large mycobags (Unicorn Bags, Plano, TX) prior to being homogenized, extracted, and partitioned with EtOAc. The EtOAc soluble material (57.5 g) was subjected to silica gel vacuum liquid chromatography (VLC) with elution steps of 1:1 hexanes/DCM, DCM, 10:1 DCM/MeOH and MeOH, yielding 4 fractions. The 10:1 DCM/MeOH fraction (8.0 g) was subjected to HP20SS VLC and eluted with a step gradient of MeOH in H_2O (30%, 50%, 70%, 90%, and 100%) and 1:1 DCM/MeOH, yielding a total of 6 fractions. Bioassay analysis of the resulting fractions revealed the *T. vaginalis*-inhibitory activity was concentrated in the MeOH fraction from HP20SS VLC. The MeOH fraction was subjected to further bioassay-guided fractionation using preparative C_{18} HPLC (250 mm × 21.2 mm, 5 μm) with a MeOH-H_2O gradient containing 0.1% HCOOH (50:50 to 100:0) to yield the known bioactive compound **46** (52.2 mg).

Borohydride Reduction of 46.

To a flask, 9.0 mg of **46** (0.016 mmol) in 4 mL MeOH was added. While stirring, 7.6 mg of sodium borohydride (0.20 mmol) dissolved in 1 mL MeOH was added slowly over a 5 min period. The reaction mixture was stirred at room temperature for 45 min. The reaction was quenched by adding 500 μL of 1M HCl to the flask and stirred for 10 min. Solvent was removed from the reaction mixture under vacuum to yield compound **47** (8.8 mg, 96% yield). ^{1}H NMR (500 MHz, $CDCl_3$): 14.44 (s, 1H), 13.94 (s, 1H), 11.91 (s, 1H), 11.44 (s, 1H), 7.04 (s, 1H), 6.70 (s, 1H), 6.47 (m, 2H), 6.08 (s, 1H), 5.04 (s, 1H), 4.74 (dd, J = 5.5, 2.0 Hz, 1H), 4.26 (dd, J = 4.0, 2.0 Hz, 1H), 3.68 (s, 3H), 3.05 (d, J = 18.0 Hz, 1H), 2.81 (m, 1H), 2.58 (d, J = 18.0 Hz, 1H), 2.40 (s, 3H), 2.37 (m, 1H), 2.12 (m, 1H), 1.91 (m, 1H). ^{13}C NMR (125 MHz, $CDCl_3$): 188.5, 186.7, 184.6, 179.4, 171.1, 161.4, 158.5, 155.9, 148.3, 147.6, 141.8, 134.9, 131.8, 117.5, 117.2×2, 111.7, 111.3, 106.5, 104.6, 100.1, 83.8, 71.9, 66.8, 53.4, 43.6, 37.6, 30.5, 24.4, 23.0, 22.4.

Purification of Tetramic Acid Derivatives 48–56.

5 fungal isolates coded Miller-1 Cz-3, Miller-26 SEA-3, KY6863 TV8–3, Column L5 SEA-1, CA9310 TV8–3, were identified as *Fusarium* sp. isolate B, *Fusarium* sp. isolate C, *Penicillium* sp., *Alternaria* sp., *Phoma* sp. P34E5, respectively, based on their ribosomal internal transcribed spacer (ITS) sequence data (GenBank accession numbers MK401898, MK401899, MK401895, MK401896, and MK401897, respectively). These five fungal

isolates were fermented on a solid-state medium composed of Cheerios breakfast cereal supplemented with 0.3% sucrose solution for 4 weeks at 25 °C. The fungal isolate designated Column L5 SEA-1 was inoculated into 16 L of PDB media (10 g/L dried mashed potato, 5 g/L glucose) supplemented with 2 g/L $NaNO_3$ and grown for 9 days with shaking.

The fungal culture designated Miller-1 Cz-3 (*Fusarium* sp. isolate B) was homogenized and partitioned 3× with equal volumes of EtOAc. The resulting EtOAc soluble material (25.0 g) was subjected to silica gel VLC with elution steps of 1:1 hexanes/DCM, DCM, 10:1 DCM/MeOH, and MeOH, yielding 4 fractions. The 10:1 DCM/MeOH fraction was subjected to HP20SS VLC and eluted with a step gradient of MeOH in H_2O (30%, 50%, 70%, 90%, and 100%), yielding 5 fractions. The 90% MeOH fraction from HP20SS VLC was further fractionated by preparative C_{18} HPLC (250 mm × 21.2 mm, 5 μm) with a MeCN-H_2O gradient containing 0.1% HCOOH (70:30 to 100:0) to yield compounds **48** (56 mg) and **49** (18.9 mg).

The fungal culture designated Miller-26 SEA-3 (*Fusarium* sp. isolate C) was homogenized and partitioned 3× with equal volumes of EtOAc. The resulting EtOAc soluble material (14.0 g) was subjected to silica gel VLC with elution steps of 1:1 hexanes/DCM, DCM, 10:1 DCM/MeOH, and MeOH, yielding 4 fractions. The 10:1 DCM/MeOH fraction was subjected to HP20SS VLC and eluted with a step gradient of MeOH in H_2O (30%, 50%, 70%, 90%, and 100%), yielding 5 fractions. The 70% MeOH fraction from HP20SS VLC was further fractionated by isocratic preparative C_{18} HPLC (250 mm × 21.2 mm, 5 μm) with MeOH-H_2O (75:25) to yield compound **50** (50 mg).

The fungal culture designated KY6863 TV8–3 (*Penicillium* sp.) was homogenized and partitioned 3× with equal volumes of EtOAc. The resulting EtOAc soluble material (31.0 g) was subjected to silica gel VLC with elution steps of 1:1 hexanes/DCM, DCM, 10:1 DCM/MeOH, and MeOH, yielding 4 fractions. The 10:1 DCM/MeOH fraction was subjected to HP20SS VLC and eluted with a step gradient of MeOH in H_2O (30%, 50%, 70%, 90%, and 100%), yielding 5 fractions. The 90% MeOH fraction from HP20SS VLC was further fractionated by preparative C_{18} HPLC (250 mm × 21.2 mm, 5 μm) with a MeOH-H_2O gradient containing 0.1% HCOOH (85:15 to 100:0) to yield compounds **51** (50 mg) and **52** (15 mg). 5'-epipyrrolocin A (**52**): pale yellow plates; $[\alpha]^{20}_{D}$ +93 (*c* 0.05, MeOH); UV (MeOH) λ_{max} (log ε) 238 (2.37), 265 (0.42), 295 (0.77); CD (MeOH) λ_{max} ($\Delta\varepsilon$) 234 (8.1), 291 (6.1); ^{1}H and ^{13}C NMR data, see Tables 1 and 2; HRESIMS *m*/*z* 456.2747 $[M - H]^-$ (calcd for 456.2755).

Fungal culture broth prepared from the fungus designated Column L5 SEA-1 (*Alternaria* sp.) was partitioned 3× with equal volumes of EtOAc to provide 3.0 g of EtOAc-soluble residue. The organic residue was subjected to HP20SS VLC and eluted with a step gradient of MeOH in H_2O (30%, 50%, 70%, 90%, and 100%), yielding 5 fractions. The 90% MeOH fraction was further fractionated by preparative C_{18} HPLC (250 mm × 21.2 mm, 5 μm) with a MeOH-H_2O gradient containing 0.1% HCOOH (90:10 to 100:0) yielding 6 fractions (Fr.1–6). Bioactive compounds in fractions 2 and 4 were further purified by isocratic semi-preparative C_{18} HPLC (250 mm × 10 mm, 5 μm) with MeCN-H_2O containing 0.1% HCOOH (80:20) to yield compounds **53** (67 mg) and **54** (7.5 mg). 5'-epibeauversetin

(**54**): pale yellow plate; $[\alpha]^{20}_{D}$ +409 (*c* 0.17, MeOH); UV (MeOH) λ_{max} (log ε) 236 (4.39), 287 (4.11); CD (MeOH) λ_{max} ($\Delta\varepsilon$) 232 (8.2), 285 (9.8); ^{1}H and ^{13}C NMR data, see Tables 1 and 2; HRESIMS *m*/*z* 398.2337, $[M - H]^{-}$ (calcd for $C_{24}H_{32}NO_4$, 398.2337).

The fungal culture designated CA9310 TV8–3 (*Phoma* sp. P34E5) was homogenized and partitioned 3× with equal volumes of EtOAc. The resulting EtOAc soluble material (38.0 g) was subjected to silica gel VLC with elution steps of 1:1 hexanes/DCM, DCM, 10:1 DCM/MeOH, and MeOH, yielding 4 fractions. The 10:1 DCM/MeOH fraction was subjected to HP20SS VLC and eluted with a step gradient of MeOH in H_2O (30%, 50%, 70%, 90%, and 100%) yielding 5 fractions. The 70% MeOH fraction from HP20SS VLC was further fractionated by isocratic preparative C_{18} HPLC (250 mm × 21.2 mm, 5 μm) with MeOH-H_2O containing 0.1% HCOOH (85:15) to yield compounds **55** (140 mg) and **56** (4 mg).

Preparation of MTPA Esters.

Compound **52** (0.5 mg) was dissolved in pyridine-d_5 and equal portions transferred to two NMR tubes.[47] The (*R*)-α-methoxy-α-trifluoromethyl-phenylacetyl chloride [(*R*)-MTPA-Cl] (5 μL) was added into one sample under an N_2 gas stream. After mixing, it was incubated at 40 °C in a H_2O bath and monitored every 2 h by ^{1}H NMR. The same method was used to treat the second sample using (*S*)-α-methoxy-α-trifluoromethyl-phenylacetyl chloride [(*S*)-MTPA-Cl] as the reagent to yield the (*R*)-Mosher ester derivative. (*S*)-Mosher ester derivative: ^{1}H NMR (500 MHz, pyridine-d_5): 6.38 (1H, m, H-14), 6.07 (1H, m, H-15), 5.90 (1H, m, H-16), 5.69 (1H, m, H-13), 3.87 (1H, m, H-12), 2.37 (1H, m, H-17), 2.10 (1H, m, H-17), 1.20 (3H, d, *J* = 6.5 Hz, CH_3-19). (*R*)-Mosher ester derivative: ^{1}H NMR (500 MHz, pyridine-d_5) 6.39 (1H, m, H-14), 6.07 (1H, m, H-15), 5.92 (1H, m, H-16), 5.72 (1H, m, H-13), 3.94 (1H, m, H-12), 2.37 (1H, m, H-17), 2.10 (1H, m, H-17), 1.19 (3H, d, *J* = 6.5 Hz, CH_3-19).

Cleavage of the Tetramic Acid Ring and Marfey's Reaction.

Samples of compounds (20 mg) were dissolved in MeOH (0.6 mL) followed by addition of 1 M NaOH (75 μL) and a NaOCl solution (available chlorine 10−15%, 0.35 mL) as per prior reports.[42–43] The mixture was stirred at room temperature for 8 h and then it was quenched by adding 1 M aqueous Na_2SO_2 (3 mL) and neutralized by the addition of 1 M HCl. After removal of the solvent, the residue was diluted with H_2O, and the resulting mixture was partitioned against EtOAc. The organic layer was retained and the solvent removed *in vacuo*. The residue was dissolved in 6 M HCl (500 μL) and held overnight at 110 °C. The solvent was removed from the hydrolysate under a stream of N_2 and the residue treated with 1 M $NaHCO_3$ (40 μL) and 1% FDAA/acetone (200 μL) at 70 °C for 1 h. The reactants were neutralized with 1 M HCl (40 μL) and diluted with MeCN (400 μL) prior to LC-ESIMS analysis. FDAA derivatives of L-Ser/*N*-Me-L-Ser and D-Ser/*N*-Me-D-Ser standards were prepared in a similar manner. Aqueous solutions of serine standards (50 mM, 50 μL) were reacted, neutralized, and diluted following the same procedure.

Supplementary Material

Refer to Web version on PubMed Central for supplementary material.

ACKNOWLEDGMENTS

Research reported in this publication was supported by the National Institutes of Health, National Institute of Allergy and Infectious Diseases (R33AI119713). The LC-ESIMS instrument used for this project was provided in part by a Challenge Grant from the Office of the Vice President for Research, University of Oklahoma, Norman Campus and an award through the Shimadzu Equipment Grant Program. We appreciate the contributions of soil samples from citizen scientists J. Miller, L. Miller, and W. Tierney to the University of Oklahoma Citizen Science Soil Collection Program, which served as the sources for several of the fungi reported in this study.

ABBREVIATIONS

SI	selectivity index
PAINS	pan-assay interference compounds
VLC	vacuum liquid chromatography
ITS	internal transcribed spacer
MTPA	α-methoxy-α-trifluoromethyl-phenylacetyl
FDAA	1-Fluoro-2–4-Dinitrophenyl-5-L-Alanine Amide
ATCC	the American Type Culture Collection

REFERENCES

(1). Sutton M, Sternberg M, Koumans EH, McQuillan G, Berman S, Markowitz L (2007) The prevalence of *Trichomonas vaginalis* infection among reproductive-age women in the United States, 2001–2004. Clin. Infect. Dis. 45, 1319–1326. DOI: 10.1086/522532. [PubMed: 17968828]

(2). Kissinger P (2015) *Trichomonas vaginalis*: a review of epidemiologic, clinical and treatment issues. BMC Infect. Dis. 15, 307. DOI: 10.1186/s12879-015-1055-0. [PubMed: 26242185]

(3). Gabriel G, Robertson E, Thin RN (1982) Single dose treatment of trichomoniasis. J. Int. Med. Res. 10, 129–130. DOI: 10.1177/030006058201000212. [PubMed: 7067925]

(4). Aubert JM, Sesta HJ (1982) Treatment of vaginal trichomoniasis. Single, 2-gram dose of metronidazole as compared with a seven-day course. J. Reprod. Med. 27, 743–745. [PubMed: 7161754]

(5). Howe K, Kissinger PJ (2017) Single-dose compared with multidose metronidazole for the treatment of trichomoniasis in women: a meta-analysis. Sex. Transm. Dis. 44, 29–34. DOI: 10.1097/olq.0000000000000537. [PubMed: 27898571]

(6). Bendesky A, Menéndez D, Ostrosky-Wegman P (2002) Is metronidazole carcinogenic? Mutat. Res. 511, 133–144. DOI: 10.1016/S1383-5742(02)00007-8. [PubMed: 12052431]

(7). Dobiás L, Černá M, Rössner P, Šrám R (1994) Genotoxicity and carciogenicity of metronidazole. Mutat. Res. 317, 177–194. DOI: 10.1016/0165-1110(94)90001-9. [PubMed: 7515153]

(8). 2015 sexually transmitted diseases treatment guidelines: trichomoniasis. https://www.cdc.gov/std/tg2015/trichomoniasis.htm (accessed June 28, 2018).

(9). Kirkcaldy RD, Augostini P, Asbel LE, Bernstein KT, Kerani RP, Mettenbrink CJ, Pathela P, Schwebke JR, Secor WE, Workowski KA, Davis D, Braxton J, Weinstock HS (2012) *Trichomonas vaginalis* antimicrobial drug resistance in 6 U.S. cities, STD Surveillance Network, 2009–2010. Emerging Infect. Dis. 18, 939–943. DOI: 10.3201/eid1806.111590.

(10). Schwebke JR, Barrientes FJ (2006) Prevalence of *Trichomonas vaginalis* isolates with resistance to metronidazole and tinidazole. Antimicrob. Agents Chemother. 50, 4209–4210. DOI: 10.1128/aac.00814-06. [PubMed: 17000740]

(11). Scopel M, dos Santos O, Frasson A, Abraham W, Tasca T, Henriques A, Macedo A (2013) Anti-*Trichomonas vaginalis* activity of marine-associated fungi from the South Brazilian Coast. Exp. Parasitol. 133, 211–216. DOI: 10.1016/j.exppara.2012.11.006. [PubMed: 23201217]

(12). Duarte M, Seixas A, de Carvalho M, Tasca T, Macedo A (2016) Amaurocine: anti-*Trichomonas vaginalis* protein produced by the basidiomycete *Amauroderma camerarium*. Exp. Parasitol. 161, 6–11. DOI: 10.1016/j.exppara.2015.12.012. [PubMed: 26706604]

(13). Desrivot J, Waikedre J, Cabalion P, Herrenknecht C, Bories C, Hocquemiller R, Fournet A (2007) Antiparasitic activity of some New Caledonian medicinal plants. J. Ethnopharmacol. 112, 7–12. DOI: 10.1016/j.jep.2007.01.026. [PubMed: 17329051]

(14). Calzada F, Yepez-Mulia L, Tapia-Contreras A (2007) Effect of Mexican medicinal plant used to treat trichomoniasis on *Trichomonas vaginalis* trophozoites. J. Ethnopharmacol. 113, 248–251. DOI: 10.1016/j.jep.2007.06.001. [PubMed: 17628366]

(15). Lara-Díaz V, Gaytán-Ramos A, Dávalos-Balderas A, Santos-Guzmán J, Mata-Cárdenas B, Vargas-Villarreal J, Barbosa-Quintana A, Sanson M, López-Reyes A, Moreno-Cuevas J (2009) Microbiological and toxicological effects of Perla black bean (*Phaseolus vulgaris* L.) extracts: *in vitro* and *in vivo* studies. Basic Clin. Pharmacol. Toxicol. 104, 81–86. DOI: 10.1111/j.1742-7843.2008.00330.x. [PubMed: 19053992]

(16). Moon T, Wilkinson J, Cavanagh H (2006) Antiparasitic activity of two *Lavandula* essential oils against *Giardia duodenalis*, *Trichomonas vaginalis*, and *Hexamita inflata*. Parasitol. Res. 99, 722–728. DOI: 10.1007/s00436-006-0234-8. [PubMed: 16741725]

(17). Kaneda Y, Tanaka T, Saw T (1990) Effects of berberine, a plant alkaloid, on the growth of anaerobic protozoa in axenic culture. Tokai J. Exp. Clin. Med. 15, 417–423. [PubMed: 2131648]

(18). Wu J, Zhang M, Ding D, Tan T, Yan B (1995) Effect of *Cladonia alpestris* on *Trichomonas vaginalis in vitro*. Chinese Journal of Parasitology and Parasitic Diseases 13, 126–129. [PubMed: 7554162]

(19). Wang H (1993) Antitrichomonal action of emodin in mice. J. Ethnopharmacol. 40, 111–116. DOI: 10.1016/0378-8741(93)90055-A. [PubMed: 8133650]

(20). Bhagwat P, Gokhale B, Sane H, Thirumalachar M (1964) Assessment of antitrichomonal activity of hamycin. Indian J. Med. Res. 52, 36–37. [PubMed: 14112160]

(21). He W, VanPuyvelde L, Maes L, Bosselaers J, DeKimpe N (2003) Antitrichomonas *in vitro* activity of *Cussonia holstii* Engl. Nat. Prod. Res. 17, 127–133. DOI: 10.1080/1478641031000103713. [PubMed: 12713125]

(22). Loyola L, Bórquez J, Morales G, Araya J, González J, Neira I, Sagua H, San-Martín A (2001) Diterpenoids from *Azorella yareta* and their trichomonicidal activities. Phytochemistry 56, 177–180. DOI: 10.1016/S0031-9422(00)00380-0. [PubMed: 11219811]

(23). Kayser O, Kiderlen A, Croft S (2003) Natural products as antiparasitic drugs. Parasitol. Res. 90, S55–S62. DOI: 10.1007/s00436-002-0768-3. [PubMed: 12937967]

(24). Newman DJ, Cragg GM (2016) Natural products as sources of new drugs from 1981 to 2014. J. Nat. Prod. 79, 629–661. DOI: 10.1021/acs.jnatprod.5b01055. [PubMed: 26852623]

(25). Campos Aldrete M, Salgado-Zamora H, Luna J, Meléndez E, Meráz-Ríos M (2005) A high-throughput colorimetric and fluorometric microassay for the evaluation of nitroimidazole derivatives anti-*Trichomonas* activity. Toxicol. in Vitro 19, 1045–1050. DOI: 10.1016/j.tiv.2005.04.007. [PubMed: 15963680]

(26). Duarte M, Giordani R, De Carli G, Zuanazzi J, Macedo A, Tasca T (2009) A quantitative resazurin assay to determinate the viability of *Trichomonas vaginalis* and the cytotoxicity of organic solvents and surfactant agents. Exp. Parasitol. 123, 195–198. DOI: 10.1016/j.exppara.2009.07.002. [PubMed: 19619538]

(27). Chen JL, Steele TWJ, Stuckey DC (2015) Modeling and application of a rapid fluorescence-based assay for biotoxicity in anaerobic digestion. Environ. Sci. Technol. 49, 13463–13471. DOI: 10.1021/acs.est.5b03050. [PubMed: 26457928]

(28). Forestier C, Späth G, Prina E, Dasari S (2015) Simultaneous multi-parametric analysis of *Leishmania* and of its hosting mammal cells: a high content imaging-based method enabling sound drug discovery process. Microb. Pathog. 88, 103–108. DOI: 10.1016/j.micpath.2014.10.012. [PubMed: 25448129]

(29). Ruelius H, Gauche A (1950) Fusarubin, a naphthoquinone coloring matter from Fusaria. Justus Liebigs Ann. Chem. 569, 38–59.

(30). Arnstein H, Cook A (1947) Production of antibiotics by fungi. Part III. Javanicin. An antibacterial pigment from *Fusarium javanicum*. J. Chem. Soc. 1947, 1021–1028.

(31). Arsenault G (1968) Fungal metabolites. III. Quinones from *Fusarium solani* D2 purple and structure of (+)-solaniol. Tetrahedron 24, 4745–4749. DOI: 10.1016/S0040-4020(01)98671-5.

(32). Kurobane IZ,N; Fukuda A (1985) New metabolites of *Fusarium martii* related to dihydrofusarubin. J. Antibiot. 39, 205–214. DOI: 10.7164/antibiotics.39.205.

(33). Hashimoto J, Motohashi K, Sakamoto K, Hashimoto S, Yamanouchi M, Tanaka H, Takahashi T, Takagi M, Shin-ya K (2009) Screening and evaluation of new inhibitors of hepatic glucose production. J. Antibiot. 62, 625–629. DOI: 10.1038/ja.2009.93.

(34). Hughes W, Gray V, Gutteridge W, Latter V, Pudney M (1990) Efficacy of a hydroxynaphthoquinone, 566C80, in experimental *Pneumocystis carinii* pneumonitis. Antimicrob. Agents Chemother. 34, 225–228. DOI: 10.1128/AAC.34.2.225. [PubMed: 2327770]

(35). Baggish A, Hill D (2002) Antiparasitic agent atovaquone. Antimicrob. Agents Chemother. 46, 1163–1173. DOI: 10.1128/AAC.46.5.1163-1173.2002. [PubMed: 11959541]

(36). Baell JB (2016) Feeling nature's PAINS: Natural products, natural product drugs, and pan assay interference compounds (PAINS). J. Nat. Prod. 79, 616–28. DOI: 10.1021/acs.jnatprod.5b00947. [PubMed: 26900761]

(37). Tabata N, Tomoda H, Matsuzaki K, Omura S (1993) Structure and biosynthesis of xanthoquinodins, anticoccidial antibiotics. J. Am. Chem. Soc. 115, 8558–8564. DOI: 10.1021/ja00072a006.

(38). Sobel J (1999) Is there a protective role for vaginal flora? Curr. Infect. Dis. Rep. 1, 379–383. [PubMed: 11095812]

(39). Ma B, Forney L, Ravel J (2012) The vaginal microbiome: rethinking health and diseases. Annu. Rev. Microbiol. 66, 371–389. DOI: 10.1146/annurev-micro-092611-150157. [PubMed: 22746335]

(40). Hunter N, Dingsdag S (2017) Metronidazole: an update on metabolism, structure-cytotoxicity and resistance mechanisms. J Antimicrob Chemoth 73, 265–279. DOI: 10.1039/jac/dkx351.

(41). Philips N, Goodwin J, Fraiman A, Cole R, Lynn D (1989) Characterization of the Fusarium toxin equisetin- the use of phenylboronates in structure assignment. J. Am. Chem. Soc 111, 8223–8231.

(42). Jadulco RC, Koch M, Kakule TB, Schmidt EW, Orendt A, He H, Janso JE, Carter GT, Larson EC, Pond C, Matainaho TK, Barrows LR (2014) Isolation of pyrrolocins A-C: cis- and trans-decalin tetramic acid antibiotics from an endophytic fungal-derived pathway. J Nat Prod 77, 2537–2544. DOI: 10.1021/np500617u. [PubMed: 25351193]

(43). Minowa NK,Y; Harimaya K; Mikawa T (1998) A degradation study of vermisporin and determination of its absolute configuration. Heterocycles 48, 1639–1642.

(44). Singh SB, Zink DL, Goetz MA, W. DA, Polishook JD, Hazuda DJ (1998) Equisetin and a novel opposite stereochemical homolog phomasetin, two fungal metabolites as inhibitors of HIV-1 integrase. Tetrahedron Lett. 39, 2243–2246. DOI: 10.1016/S0040-4039(98)00269-X.

(45). Marfori E, Kajiyama S, Fukusaki E, Kobayashi A (2002) Trichosetin, a novel tetramic acid antibiotic produced in dual culture of *Trichoderma harzianum* and *Catharanthus roseus* Callus. Z. Naturforsch., C: Biosci. 57, 465–470. DOI: 10.1515/znc-2002-5-611.

(46). Neumann K, Kehraus S, Gütschow M, König G (2009) Cytotoxic and HLE-inhibitory tetramic acid derivatives from marine-derived fungi. Nat. Prod. Commun. 4, 347–354. [PubMed: 19413111]

(47). Seco JM, Quiñoá E, Riguera R (2001) A practical guide for the assignment of the absolute configuration of alcohols, amines and carboxylic acids by NMR. Tetrahedron: Asymmetry 12, 2915–2925. DOI: 10.1016/S0957-4166(01)00508-0.

(48). Yamada S, Hongo C, Yoshioka R, Chibata I (1983) Method for the racemization of optically active amino acids. J. Org. Chem 48, 843–846. DOI: 10.1021/jo00154a019.

(49). Fujii K, Ikai Y, Oka H, Suzuki M, Harada K (1997) A nonempirical method using LC/MS for determination of the absolute configuration of constituent amino acids in a peptide- combination of Marfey's method with mass spectrometry and Its practical application. Anal. Chem. 69, 5146–5151. DOI: 10.1021/ac970289b.

(50). Ratnaweera P, de Silva E, Williams D, Andersen R (2015) Antimicrobial activities of endophytic fungi obtained from the arid zone invasive plant *Opuntia dillenii* and the isolation of equisetin, from endophytic *Fusarium* sp. BMC Complement. Altern. Med. 15, 220. DOI: 10.1186/s12906-015-0722-4. [PubMed: 26160390]

(51). Putri S, Kinoshita H, Ihara F, Igarashi Y, Nihira T (2010) Ophiosetin, a new tetramic acid derivative from the mycopathogenic fungus *Elaphocordyceps ophioglossoides*. J. Antibiot. 63, 195–198. DOI: 10.1038/ja.2010.8.

(52). Baell J, Nissink J (2018) Seven year itch: pan-assay interference compounds (PAINS) in 2017-utility and limitations. ACS Chem. Biol. 13, 36–44. DOI: 10.1021/acschembio.7b00903. [PubMed: 29202222]

(53). Davids B, Gillin F, Methods for *Giardia* culture, cryopreservation, encystation, and excystation *in vitro*. In Giardia A Model Organism, Luján H; Svärd S, Eds. SpringerWienNewYork: Wien, Austria, 2011; pp 381–394.

(54). Paget T, Lloyd D (1990) *Trichomonas vaginalis* requires traces of oxygen and high concentrations of carbon dioxide for optimal growth. Mol. Biochem. Parasitol. 41, 65–72. DOI: 10.1016/0166-6851(90)90097-6. [PubMed: 2117256]

(55). Du L, Risinger A, King J, Powell D, Cichewicz R (2014) A potent HDAC inhibitor, 1-alaninechlamydocin, from a *Tolypocladium* sp. induces G2/M cell cycle arrest and apoptosis in MIA PaCa-2 cells. J. Nat. Prod. 77, 1753–1757. DOI: 10.1021/np500387h. [PubMed: 24999749]

(56). Hansen M, Nielsen S, Berg K (1989) Re-examination and further development of a precise and rapid dye method for measuring cell growth/cell kill. J. Immunol. Methods 119, 203–210. DOI: 10.1016/0022-1759(89)90397-9. [PubMed: 2470825]

(57). Fieser L (1928) The tautomerism of hydroxy quinones. J. Am. Chem. Soc. 50, 439–465. DOI: 10.1021/ja01389a033.

(58). Sreelatha T, Kandhasamy S, Dinesh R, Shruthy S, Shweta S, Mukesh D, Karunagaran D, Balaji R, Mathivanan N, Perumal PT (2014) Synthesis and SAR study of novel anticancer and antimicrobial naphthoquinone amide derivatives. Bioorg. Med. Chem. Lett. 24, 3647–3651. DOI: 10.1016/j.bmcl.2014.04.080. [PubMed: 24913712]

(59). Burns C, Gill M, Saubern S (1991) Pigments of fungi. XXI Synthesis of (±)-6-demethoxyaustrocortirubin. Aust. J. Chem. 44, 1427–1445. DOI: 10.1071/CH9911427.

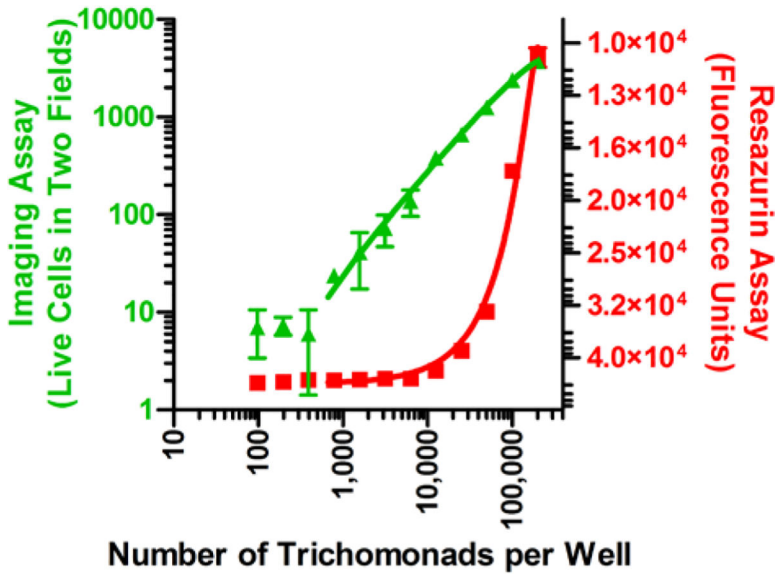

Figure 1.

Comparison of detection methods, resazurin fluorescence assay (red squares) and the newly developed imaging-based assay (green triangles, two fields per well), for measuring live versus dead trichomonads. The imaging method's limit of detection was ~1,000 trichomonads per well. In comparison, the resazurin assay detection limit was ~10,000 organisms per well.

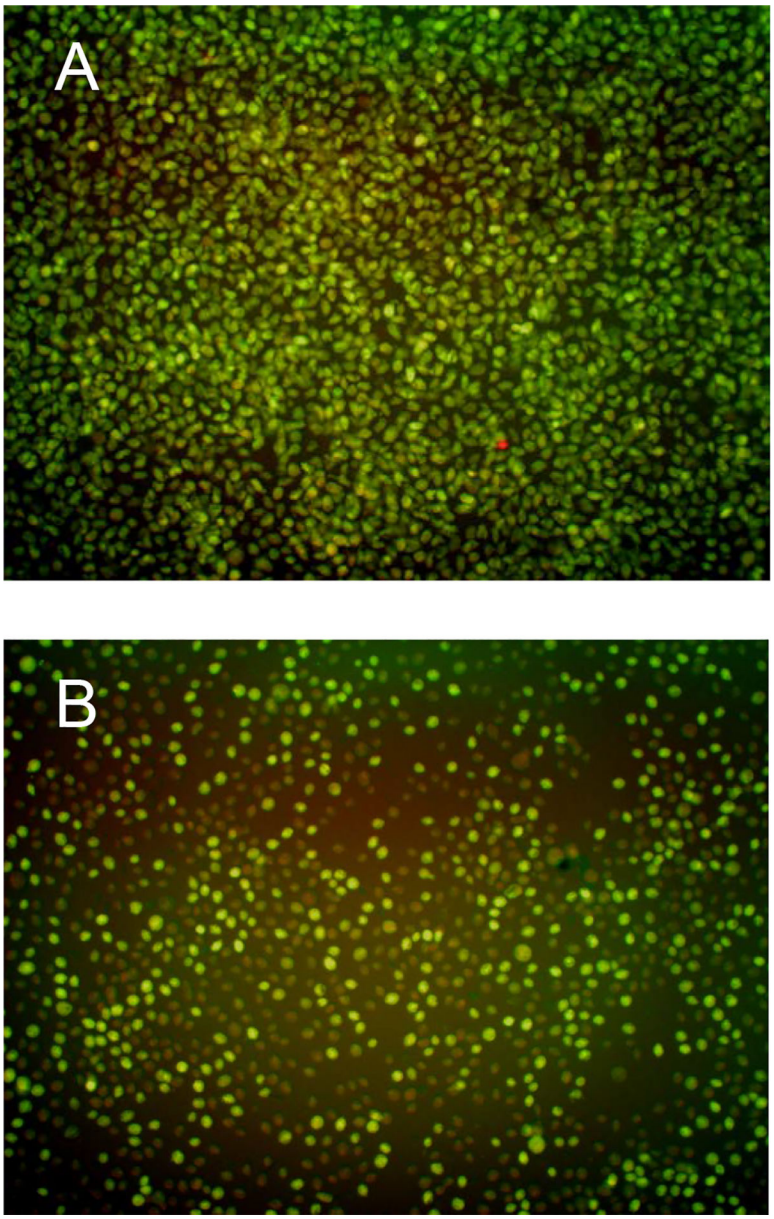

Figure 2.

(A) Sample image produced with the Operetta showing the effects of fixing and staining (0.5% glutaraldehyde, 2.5 μM propidium iodide, and 2.5 μM acridine orange) a confluent *T. vaginalis* culture at 17 h. (B) Sample image showing the effects of a fungal extract causing partial inhibition of *T. vaginalis* at 17 h. Note the fewer number of cells, the rounded appearance of the remaining cells, as well as the large number of rust colored cells (the rust color is due to the overlay of green and red emission channels) indicating that a majority of the remaining *T. vaginalis* cells are dead or dying.

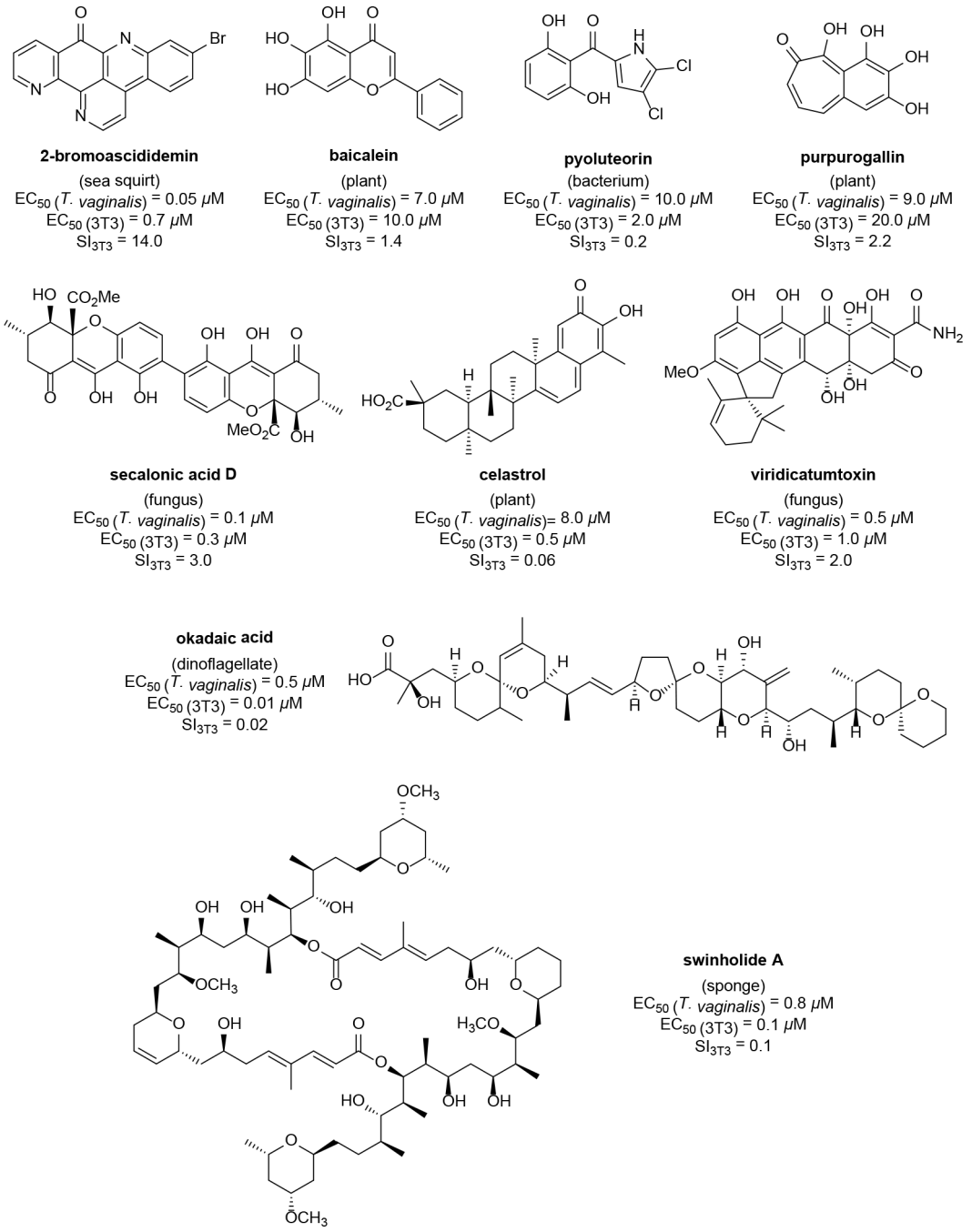

Figure 3.

Results from screening 430 purified natural products against *T. vaginalis* in the imaging-based parasite viability assay. The structures of the 9 most active metabolites are illustrated along with their EC_{50} values against both the parasite and a mammalian cell line (3T3 fibroblasts). Based on those data, a SI_{3T3} value was calculated for each compound. Whereas most of the compounds exhibited near equipotent activities against both targets, 2-bromoascididemin exhibited a SI_{3T3} value of 14.0, which was the first semiselective natural product detected using this screening system.

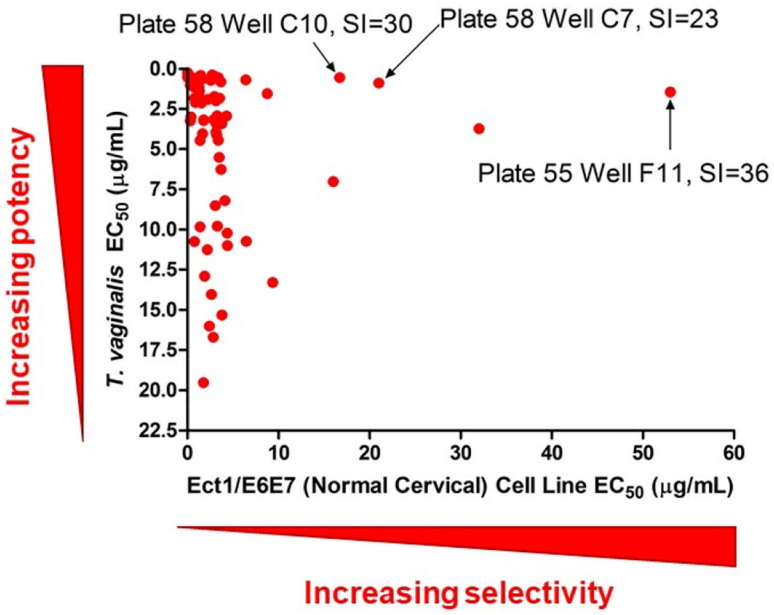

Figure 4.

Prioritization scheme for selecting potent and selective bioactive fungal extracts. After an initial pool of 1,748 fungal extracts was tested, 71 of samples were identified as being more active than 25 μM metronidazole and exhibited sigmoidal concentration-response curves against *T. vaginalis*. The fungi responsible for generating the three active samples indicated in the chart by arrows were selected for bioassay-guided fractionation studies and the bioassay results for the resulting natural products are described in this communication.

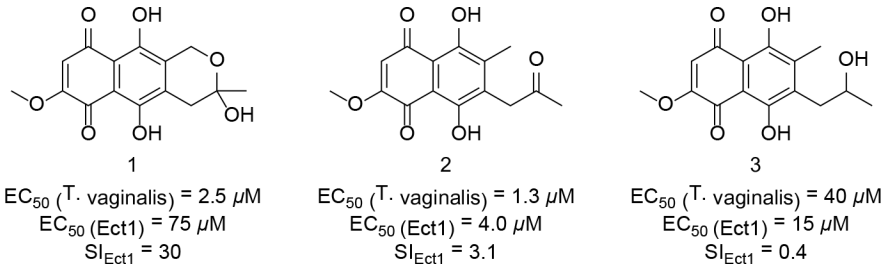

Figure 5.

Structures of metabolites **1–3** from *F. solani.* EC_{50} values for each compound against *T. vaginalis* and Ect1 cells are provided in the figure along with their calculated SI_{Ect1} values.

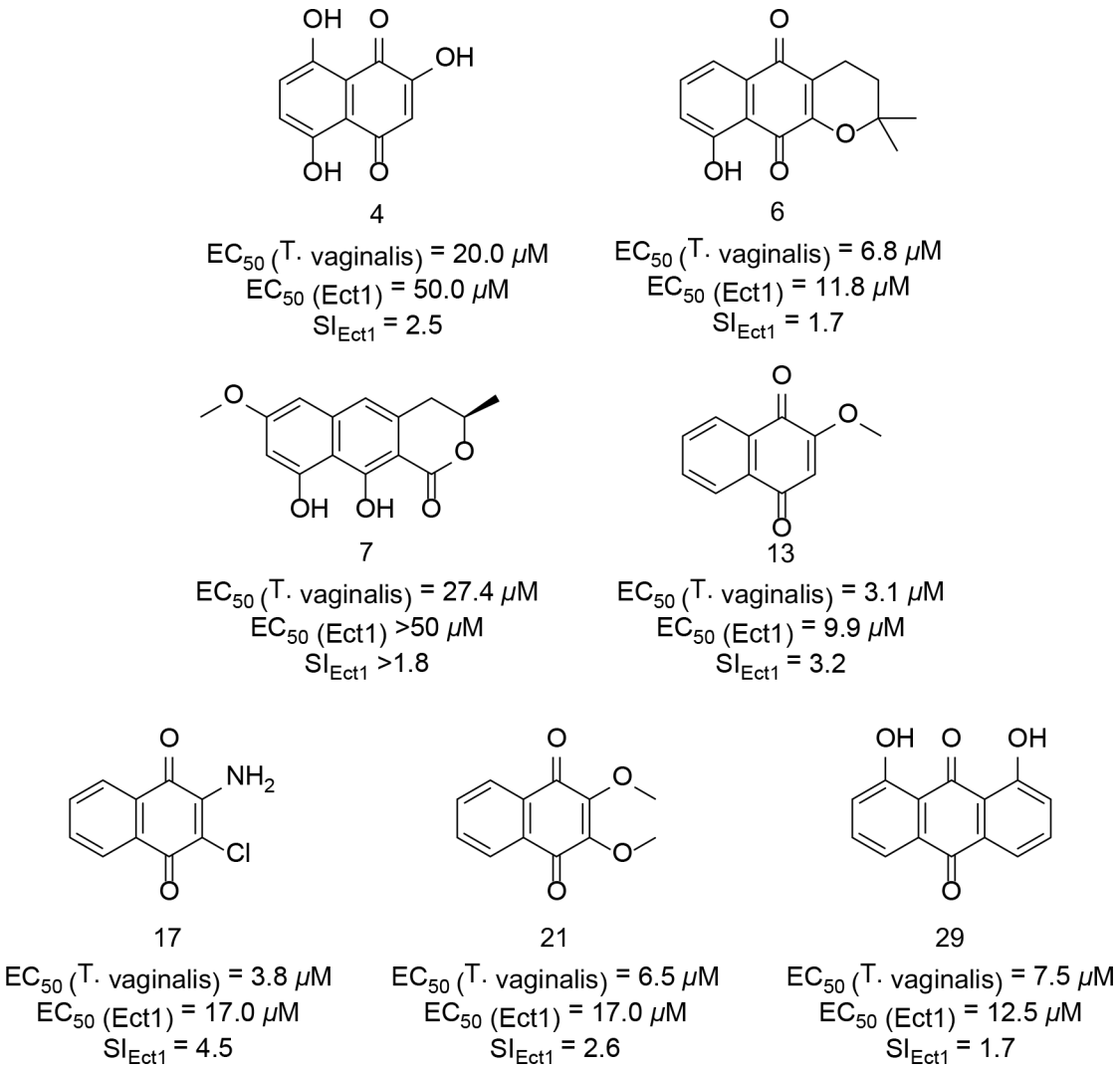

Figure 6.

Structures and biological activity of synthetic and commercially available quinone-containing compounds that exhibited SI_{Ect1} >1. EC_{50} values for each compound against *T. vaginalis* and Ect1 cells are provided in the figure along with their calculated SI_{Ect1} values.

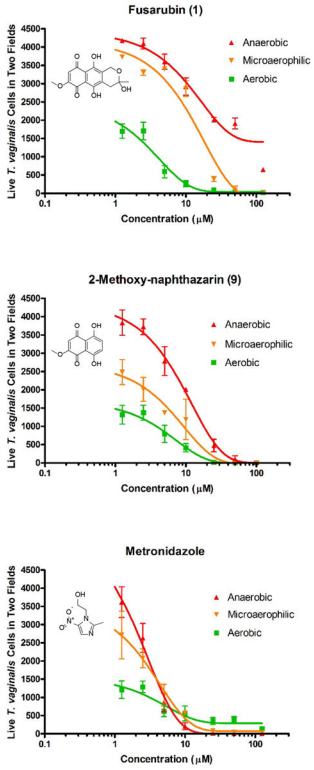

Figure 7.

Testing the effects of varying oxygen levels on the antitrichomonal activities of fusarubin (**1**), 2-methoxynaphthazarin (**9**), and metronidazole using the imaging assay [data are expressed as the mean of two visual fields per well performed in triplicate ± SD; DMSO (vehicle) did not exceed 1% by volume].

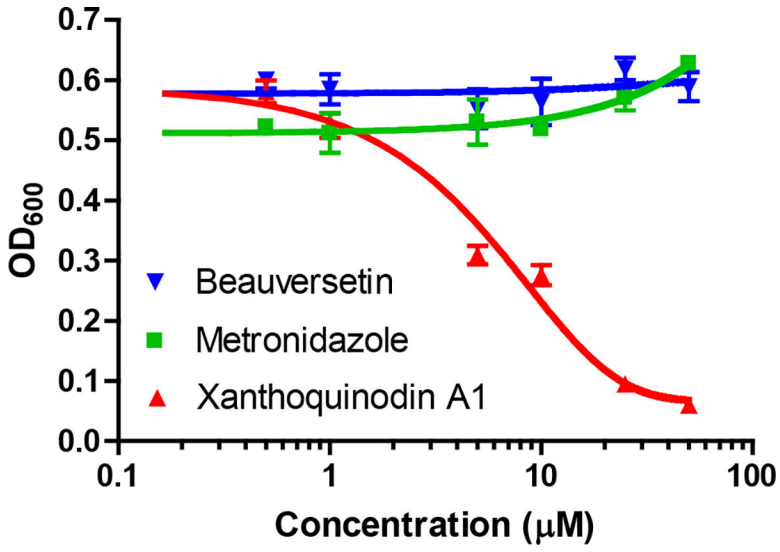

Figure 8.

Effect of selected compounds [beauversetin (**53**), xanthoquinodin A1 (**46**), and metronidazole] on the growth and viability of *L. acidophilus* grown under anaerobic conditions. The tetramic-acid-containing compound (**53**) had no effect on the bacterium at the concentrations tested. In contrast, **46** exhibited significant inhibition of this important member of the vaginal microflora [data are expressed as the mean of triplicate experiments ± SD; DMSO (vehicle) did not exceed 1% by volume].

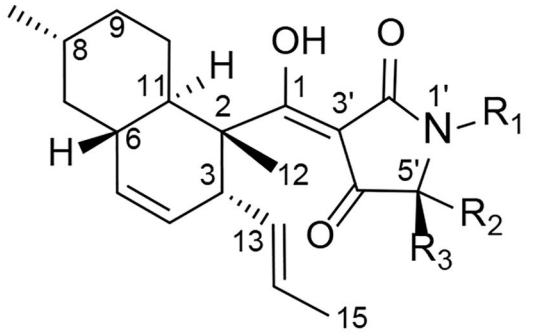

48: $R_1 = CH_3$, $R_2 = H$, $R_3 = CH_2OH$
49: $R_1 = CH_3$, $R_2 = CH_2OH$, $R_3 = H$
50: $R_1 = H$, $R_2 = H$, $R_3 = CH_2OH$

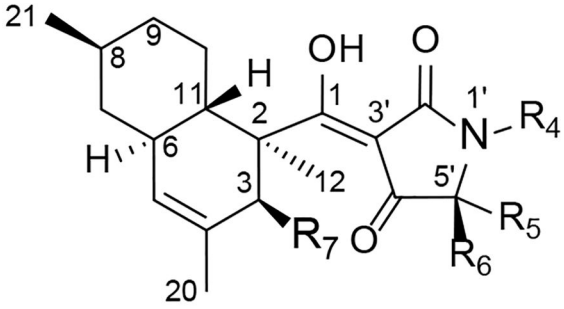

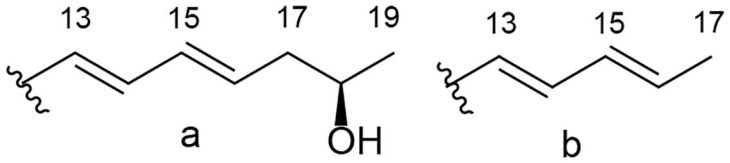

51: $R_4 = CH_3$, $R_5 = CH_2OH$, $R_6 = H$, $R_7 = a$
52: $R_4 = CH_3$, $R_5 = H$, $R_6 = CH_2OH$, $R_7 = a$
53: $R_4 = H$, $R_5 = CH_2OH$, $R_6 = H$, $R_7 = b$
54: $R_4 = H$, $R_5 = H$, $R_6 = CH_2OH$, $R_7 = b$
55: $R_4 = CH_3$, $R_5 = CH_2OH$, $R_6 = H$, $R_7 = b$
56: $R_4 = CH_3$, $R_5 = H$, $R_6 = CH_2OH$, $R_7 = b$

Figure 9.
Structures of tetramic-acid-containing metabolites **48–49** from *Fusarium* sp. isolate B, **50** from *Fusarium* sp. isolate C, **51–52** from *Penicillium* sp., **53–54** from *Alternaria* sp., and **55–56** from *Phoma* sp. P34E5.

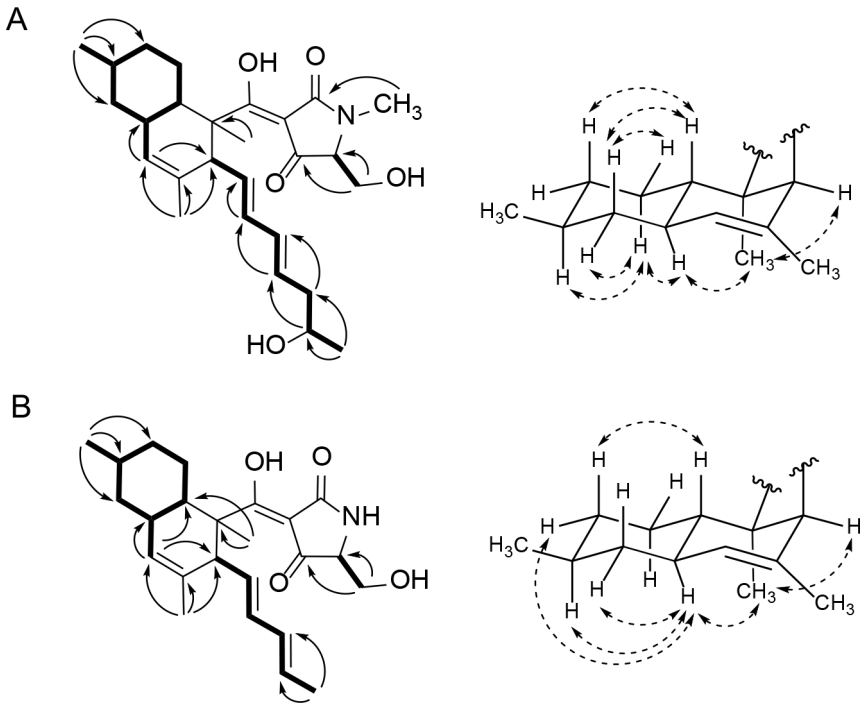

Figure 10.

Key ^{1}H-^{1}H COSY (left side – bold bonds), ^{1}H-^{13}C HMBC (left side – single-headed arrows), ^{1}H-^{1}H ROESY (right side – double headed arrows) correlations for compounds **52** (A) and **54** (B).

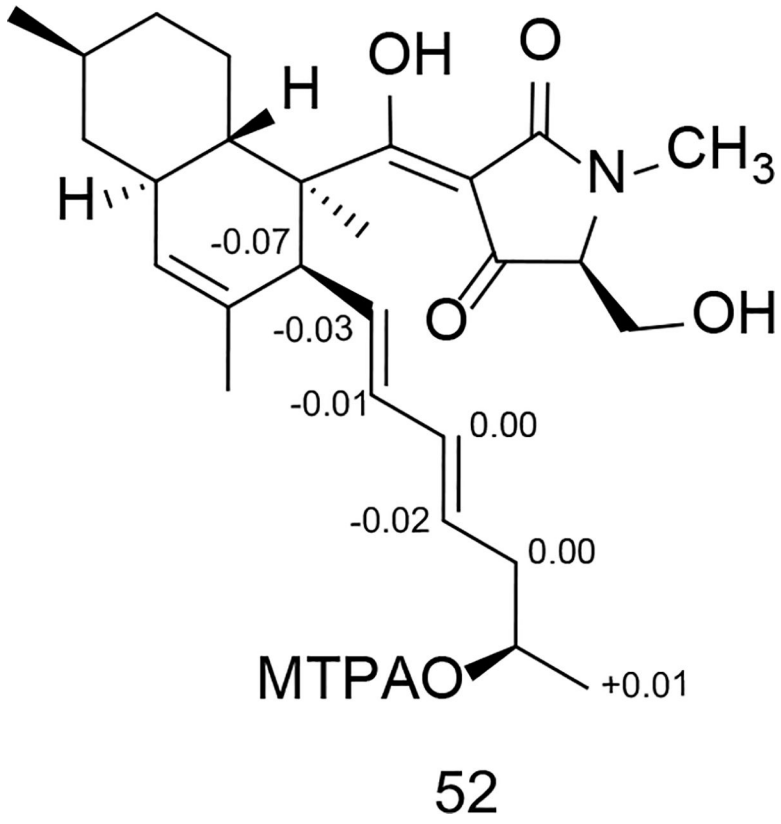

Figure 11.

$\Delta\delta_{S\text{-}R}$ values obtained in pyridine-d_5 of the MTPA esters for compound **52**.

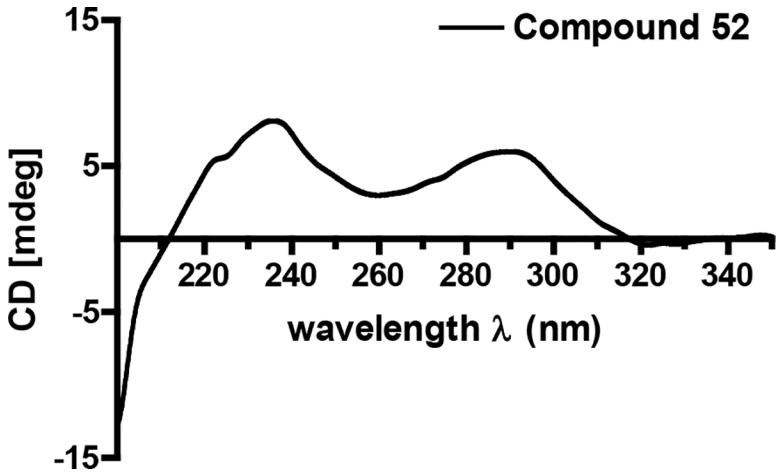

Figure 12.
Circular dichroism (ECD) spectrum for compound **52**.

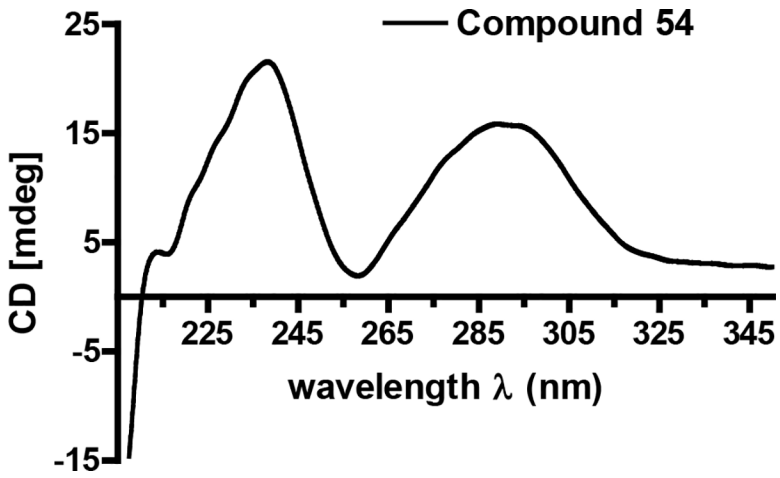

Figure 13.
Circular dichroism (ECD) spectrum for compound **54**.

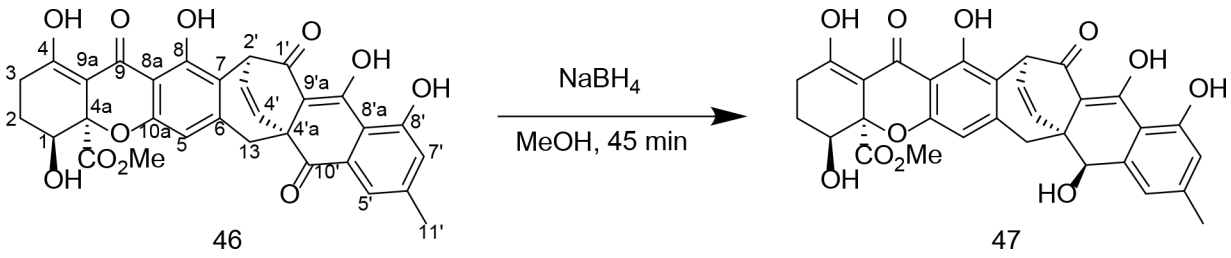

46 47

Scheme 1.

Structure of xanthoquinodin A1 (**46**) from the *H. grisea* isolate. The compound was subjected to $NaBH_4$ reduction leading to the stereoselective generation of the new secondary-alcohol-containing product **47**.

Table 1.

^{1}H NMR data of compounds 51–54 in DMSO-d_6

Position	δ_H (J in Hz)			
	51[a]	**52**[a]	**53**[b]	**54**[b]
3	3.15, m	3.25, m	3.20, m	3.21, m
5	5.19, s	5.18, s	5.19, s	5.17, s
6	1.79[c]	1.78[c]	1.79[c]	1.78 [c]
7ax	0.82, m	0.81, m	0.80, m	0.80, m
7eq	1.78[c]	1.77[c]	1.77[c]	1.77 [c]
8	1.49, m	1.48, m	1.48, m	1.48, m
9ax	1.70, m	1.70, m	1.70, m	1.70, m
9eq	1.01[c]	1.00[c]	1.01, m	0.97, m
10ax	1.00[c]	0.98[c]	0.95, m	0.94, m
10eq	1.89, m	1.90, m	1.93, m	1.93, m
11	1.57, m	1.57, m	1.54, m	1.53, m
12	1.33, s	1.36, s	1.33, s	1.35, s
13	5.22, m	5.16, m	5.15, m	5.11, dd (10.4, 14.7)
14	5.71, m	5.79[c]	5.72, dd (10.5, 14.7)	5.78, dd (10.5, 14.7)
15	5.88, m	5.82[c]	5.90, dd (10.5, 13.7)	5.86, dd (10.5, 13.7)
16	5.50, m	5.46, m	5.50, m	5.46, m
17	2.00, m	1.99, m	1.63, d (6.5)	1.62, d (6.5)
	2.09, m	2.08, m		
18	3.57, m	3.57, m	1.52, s	1.51, s
19	0.98, d (6.0)	0.98, d (6.0)	0.88, d (6.3)	0.88, d (6.3)
20	1.52, s	1.52, s		
21	0.88, d (6.5)	0.88, d (6.5)		
1'			9.25, s	9.05, s
5'	3.75, br s	3.71[c]	3.80, br s	3.78, br s
6'	3.81, d (11.0)	3.81, m	3.63, dd (2.1, 11.0)	3.67, dd (2.1, 11.0)
	3.69, m	3.72[c]	3.59, m	3.61, m
***N*-Me**	2.92, s	2.91, s		

[a] Recorded at 500 MHz

[b] Recorded at 400 MHz

[c] Overlapped signals determined from HSQC correlations.

Table 2.

^{13}C NMR data for compounds 51–54 in DMSO-d_6 (100 MHz, δ in ppm)

	δ_C			
Position	**51**	**52**	**53**	**54**
1	195.9	196.5	199.0	199.0
2	49.0	49.6	49.2	49.5
3	49.2	48.6	48.5	48.1
4	131.3	131.9	131.4	131.6
5	126.4	126.1	126.0	125.7
6	39.1	39.2	38.7	38.7
7	42.4	42.5	42.1	42.2
8	33.3	33.4	33.0	33.0
9	35.8	35.9	35.5	35.5
10	28.1	28.1	27.6	27.7
11	39.4	39.9	39.3	39.3
12	14.0	14.2	13.4	13.5
13	130.9	131.4	130.5	130.6
14	132.7	133.0	132.1	132.5
15	131.8	132.0	131.1	131.6
16	130.9	130.5	128.0	127.7
17	42.7	42.8	17.8	17.9
18	66.3	66.3		
19	23.5	23.5		
20	22.6	22.7	22.2	22.3
21	22.8	22.9	22.5	22.5
2’	176.6	175.8	179.2	179.0
3’	100.9	101.6	99.4	99.8
4’	190.9	190.5	190.7	190.6
5’	68.1	67.4	63.2	62.9
6’	58.4	58.6	60.8	60.7
***N*-Me**	27.2	27.3		

Table 3.

Bioassay results for the tetramic-acid-containing metabolites 48–56 including compound sources, as well as EC_{50} and SI index values

Fungal Isolate Code	Isolate Identity from ITS	Compound	Assay (EC_{50} Data in μM)				Selectivity Index Value (SI)		
			T. vaginalis	3T3 Mouse Fibroblast	Ect1 Normal Cervical	*L. acidophilus*	SI_{3T3}	SI_{Ect1}	$SI_{L.\ acid}$
Miller-1 Cz-3	*Fusarium* sp. isolate B	equisetin (**48**)	3.0	100	35	>50	33	12	>17
		5’-epiequisetin (**49**)	Inactive	nt	nt	nt	nt	nt	nt
Miller-26 SEA-3	*Fusarium* sp. isolate C	trichosetin (**50**)	2.5	30	34	>50	12	14	>20
KY6863 TV8-3	*Penicillium* sp.	pyrrolocin A (**51**)	0.060	6	10	>50	100	167	>833
		5’-epipyrrolocin A (**52**)	Inactive	nt	nt	nt	nt	nt	nt
Column L5 SEA-1	*Alternaria* sp.	beauversetin (**53**)	0.80	35	35	>50	44	44	>62
		5’-epibeauversetin (**54**)	Inactive	nt	nt	nt	nt	nt	nt
CA9310 TV8-3	*Phoma* sp.	phomasetin (**55**)	0.35	10	7	>50	29	20	>142
		5’-epiphomasetin (**56**)	Inactive	nt	nt	nt	nt	nt	nt

nt: not tested